Consumers Energy

A CMS Energy Company

Palisades Nuclear Plant
27780 Blue Star Memorial Highway
Covert, MI 49043

Tel: 616 764 2276
Fax: 616 764 3265

Nathan L. Haskell
Director, Licensing and
Performance Assessment

November 3, 2000

U.S. Nuclear Regulatory Commission
ATTN: Document Control Desk
Washington, DC 20555-0001

DOCKET 50-255 - LICENSE DPR-20 - PALISADES PLANT
Reply to Request for Additional Information Related to Revised Incore Monitoring Code, PIDAL-3, and Changes in Incore Detectors (TAC No. MA8695)

By letters dated April 21 and August 11, 2000, Consumers Energy Company forwarded a report entitled, "The PIDAL-3 Full Core System", dated February 2000, and requested NRC staff review and approval. The submittal discusses our decision to (1) replace CASMO-3 with CASMO-4, (2) reduce the number of incore detectors required to be operable from 75 percent to 50 percent, and (3) eliminate seven incore detector strings starting in operating cycle 15. By NRC letter dated September 14, 2000, the staff has requested additional information concerning these submittals. Enclosed is the response to this request.

SUMMARY OF COMMITMENTS

This letter contains no new commitments and no revisions to existing commitments.

Nathan L. Haskell, Director
Licensing and Performance Assessment

CC Administrator, Region III, USNRC
Project Manager, NRR, USNRC
NRC Resident Inspector - Palisades

Attachment

A001

ATTACHMENT

CONSUMERS ENERGY COMPANY
PALISADES PLANT
DOCKET 50-255

November 3, 2000

Reply to Request for Additional Information Related to Revised Incore Monitoring Code, PIDAL-3, and Changes in Incore Detectors (TAC No. MA8695)

55 Pages
(including the 32 page PIDAL-3 Uncertainty Analysis Manual)

REQUEST FOR ADDITIONAL INFORMATION REGARDING PALISADES' REVISED INCORE MONITORING CODE, PIDAL-3, AND CHANGES IN INCORE DETECTORS

NRC Question No. 1

The third paragraph of the April 21, 2000, cover letter mentions the licensee's intent to re-use incore detectors. Please clarify how this intent is to be accomplished.

Response to Question No. 1

Since cycle one, Palisades has been unsuccessful in reinserting Incore detectors for multiple cycle use. This differs from all of the other Combustion Engineering NSSS plants, which reinsert detectors for approximately two to three cycles of operation. Palisades has a unique upper guide structure design with arduous instrument guide tube paths that make it difficult to insert detectors. We were marginally successful in reinserting six detectors prior to cycle 7; though the effort was very costly from a dose and critical path time standpoint. Palisades decided to discontinue incore reuse at that time, but continued to investigate options for reinsertion, since replacing detectors each cycle cost Palisades approximately one million dollars plus disposal costs.

For the last two cycles, we have been testing a remote tool designed by ABBCE (now Westinghouse) to reinsert the irradiated detectors. It is our intent to reinsert the detector strings from the current cycle 15 core into the cycle 16 core during the upcoming spring refueling outage in 2001. We are confident that the reinserted detectors will operate correctly throughout cycle 16, assuming a successful reinsertion campaign. Our experience indicates that any detector failures due to handling will surface within the first month of power operation. Since there is some risk that reinserted detectors may have a higher failure rate than new detectors, we are asking for the change in the minimum number of operable detectors from 75% of 43 strings (160 total detectors) to 50% of 36 strings (90 total detectors). The uncertainty analysis provided in the April 21, 2000 submittal demonstrates that reducing the required number of operable detectors is technically justified and does not reduce our margin of safety.

NRC Question No. 2

Section 1.0 (fifth paragraph) of the report discusses the decision to eliminate seven detectors starting in fuel cycle 15. Although these detectors may not be needed with respect to PIDAL-3 evaluations, the accumulated data from a given position could provide a measured value of an outer assembly power and therefore be useful in the source estimate of the neutron fluence calculations. Please provide a technical justification for the removal of these detectors. The justification should also explain how an unexpected core-wide symmetric power redistribution towards the outer core region would be detected without these seven detectors.

Response to Question No. 2

As stated, these seven detectors are not necessary for operability of the Incore Monitoring System (PIDAL-3). The sole purpose of the Incore Monitoring System is to perform the Technical Specification surveillances required to monitor peaking factors. Since these detectors are located along the outside of the core in very low power regions, they provide no significant data for the surveillances.

However, these detectors have been useful in benchmarking very low leakage core designs using the PIDAL-3 System. Since we now have six cycles of low leakage core data from cycles 9 through 14 using several different types of shield assemblies, we are confident that SIMULATE-3 can continue to accurately predict these peripheral assembly powers. From a reactor vessel fluence standpoint, the eight assemblies shielding the six critical axial weld locations at 0° and 60° for cycle 15 and beyond are already in non-instrumented locations. Therefore, the Incore Monitoring System cannot directly measure these assembly powers. Please refer to Figure 1 "Cycle 15 Core Loading Pattern" indicating the location of the eight shield assemblies, designated NS1-NS8. At this time, we have no plans to introduce further neutron flux reductions using techniques beyond our present scope of experience.

If Palisades were to experience an unexpected redistribution of power towards the outer core region, specifically an Axial Offset Anomaly (AOA), we would immediately recognize it via our continuous on-line PIDAL monitoring. This is based on the inevitable deviations that would be seen between the detector signals and the SIMULATE-3 rhodium reaction rates. Assuming we ran for significant periods of time with an anomaly (within COLR limits), we would collect data throughout the operating cycle to rebenchmark SIMULATE-3 to account for this redistribution. The SIMULATE-3 model would need to account for this effect in order for the cycle

specific PIDAL-3 Uncertainty Analysis to be bounded by the current COLR limits (or result in a necessary revision to the COLR limits and/or a change to the next cycle's fuel design). This analysis is performed at the end of the cycle prior to releasing fluence data to Westinghouse for analysis. In the unlikely event of an unexpected redistribution of power towards the outer core region, or if we introduce shield assemblies beyond our experience base, we would evaluate the need to insert detectors back into those peripheral locations to verify the models are correct.

Figure 1 Cycle 15 Core Loading Pattern

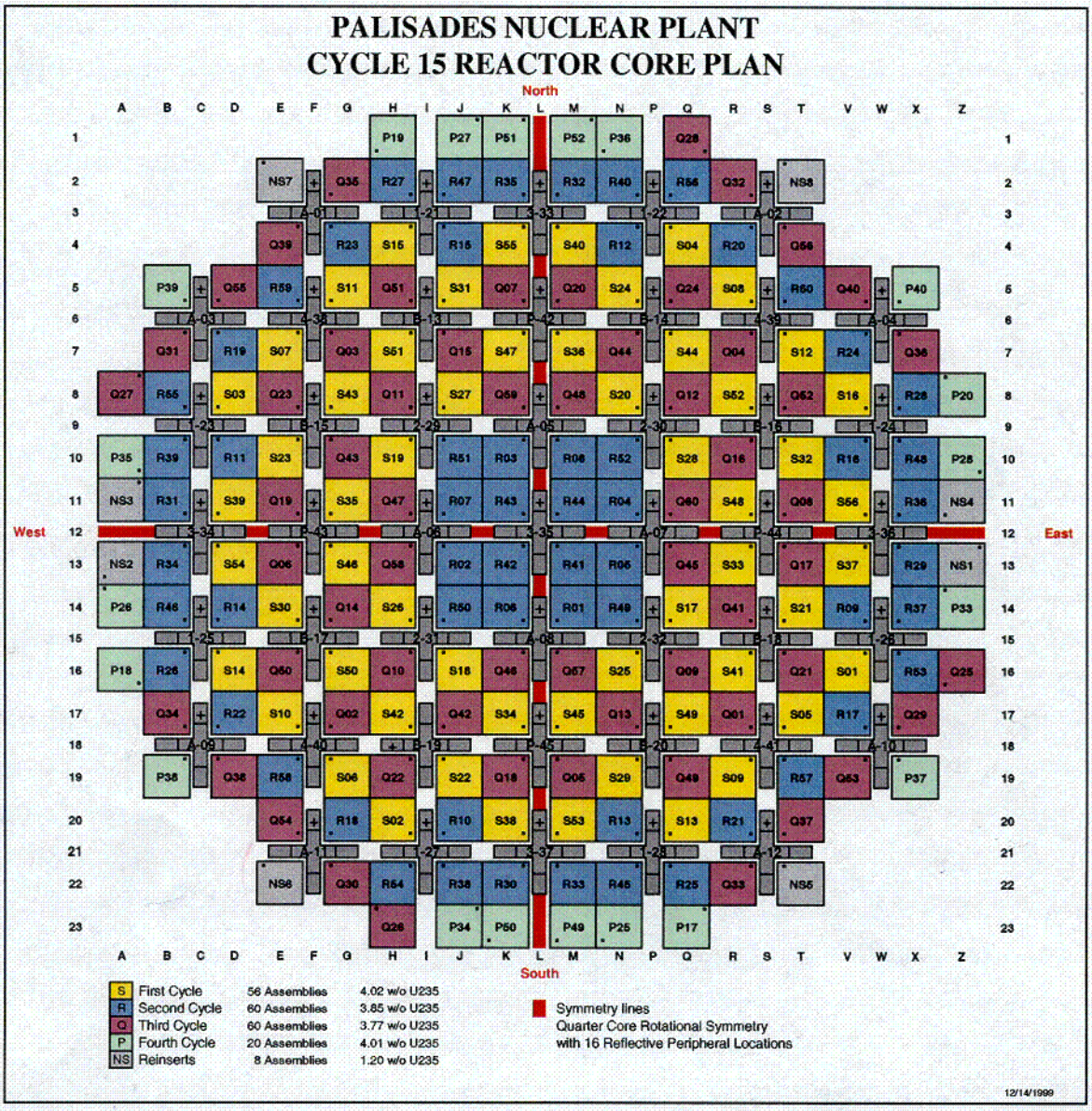

C1

NRC Question No. 3

Section 1.0 (fifth and sixth paragraphs) of the report discusses reducing the number of operable detectors from 75 percent to 50 percent. Please provide a quantitative technical justification in support of this reduction. This justification should also discuss the ability of the remaining detectors to detect

a) misaligned control rods (i.e., misalignment greater than that included in the analysis),

b) quadrant power tilts, even if greater than the Technical Specification limit, and

c) misloaded fuel.

Response to Question No. 3

The attached Figures 1 through 8 provide quantitative support for the reduction in operable detectors from 75% of 43 strings to 50% of 36 strings. All of the following tests were run using cycle 14 core design, since it is representative of the cores we are designing today. The information is laid out as follows:

Figure 1 provides the assembly relative power fractions (RPFs) for each detector location and control rod configuration. For example, "ARO" is "All Rods Out" RPFs, and "A-07" is A-07 fully inserted with all other control rods fully withdrawn. This figure provides RPF data for every control rod in quadrant 4. Which quadrant is chosen is arbitrary, since all the cores are loaded with quarter core symmetry. Refer to the April 21, 2000, PIDAL-3 submittal Figure 2.1 for locations of each detector, and to Figure 1.3 for locations of pertinent assembly and control rod locations. The Tables at the bottom of Figures 1 through 8 provide the quadrant power tilt fractions for each case. The quadrants are numbered as follows:

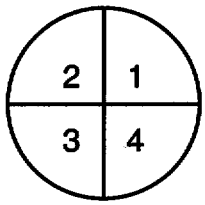

Figure 2 provides the percent deviations for Figure 1 between ARO and each individual control rod fully inserted. Figure 3 also provides the assembly RPFs for each detector location and control rod configuration. In these tests each control rod was inserted to 120 inches withdrawn. Fully withdrawn is 131 inches. Figure 4

provides the percent deviations for Figure 3 between ARO and each individual control rod inserted to 120 inches withdrawn. Figure 5 provides the assembly RPFs for each detector location and control rod 4-41 configuration. In these tests control rod 4-41 was mis-aligned up and down as much as 16 inches from the power dependent insertion limit (PDIL). Bank 4 is our lead regulating bank, and PDIL for bank 4 is 99 inches withdrawn at HFP. Figure 6 provides the percent deviations for Figure 5 between PDIL and control rod 4-41 mis-aligned around PDIL.

Figure 7 provides the assembly RPFs for each detector location and hypothetical assembly mis-loadings. In these tests new assemblies R-13, R-41, R-49, and R-57 were mis-rotated. Assembly R-41 was mis-loaded as a sub-batch R1 fuel type with no burnable poison. In the last three tests two batch P, Q, and R assemblies were swapped. Figure 8 provides the percent deviations for Figure 7 between the base case and each hypothetical mis-loading.

a) Palisades does not rely upon the Incore Monitoring System to detect mis-aligned or dropped control rods. The plant operators rely upon other independent means of verifying control rod positions.

However, as expected, the results in Figure 2 indicate that a dropped control rod has a relatively large impact on the power distribution regardless of location due to the large impact on quadrant power tilt. Therefore, this event would be recognizable regardless of the number of operable detectors.

The results in Figure 4 indicate that a mis-aligned control rod from ARO to 120 inches withdrawn is a highly localized event that would affect only the top level detectors adjacent to the mis-aligned control rod. The results in Figure 6 indicate that a bank 4 control rod mis-aligned around PDIL is also a highly localized event affecting only the detectors adjacent to the control rod. Though these events are highly localized, decreasing the number of operable detectors from 160 in 43 locations to 90 in 36 locations will not significantly impact our ability recognize these events, since SIMULATE-3 receives each control rod position from the plant computer (same as the operators). The full core SIMULATE-3 model then runs the control rod mis-alignment event and feeds the proper data to PIDAL-3 to accurately monitor the peaking factors.

b) Again, Palisades does not rely upon the Incore Monitoring System to detect quadrant power tilts (QPTs). Palisades utilizes the Excore Monitoring System to monitor QPTs, and PIDAL-3 to calibrate the excores to incores.

However, the April 21, 2000, submittal and the additional data provided show that PIDAL-3 is accurate for QPTs well beyond the Technical Specification limit of 5% at Hot Full Power (HFP) operation. From the QPT Table at the bottom of Figure 1, most dropped control rods produced QPTs larger than the Technical Specification limit of 5% at HFP. As the results indicate, any impact on QPT larger than 5% at HFP would be easily recognized throughout the core with a minimum of 90 operable detectors. Again, because SIMULATE-3 can model dropped control rods, PIDAL-3 can accurately monitor the peaking factors.

c) The results in Figure 8 indicate that mis-rotations and assembly swaps have a relatively small impact on the power distribution unless a burnable poison loaded assembly is involved. Assemblies R-41 and R-29 have burnable poison loadings, therefore any mis-loading of gadolinia or swapping with non-gadolinia assemblies would be recognizable regardless of the number of operable detectors. It should be noted that Palisades has administrative controls in place to prevent mis-loadings, and we have never mis-loaded a core. Several procedures control the fuel shuffle, core verification after the shuffle, and startup physics testing. Each undergoes rigorous reviews before closeout and release of the plant for power operation. In addition, Siemens has significantly improved their fuel pin loading procedures to prevent mis-loadings of fuel and burnable absorber pins.

Overall, the results indicate that it is the magnitude of the perturbation and its affect on quadrant power tilt, not the number of operable detectors that determines the effectiveness of the PIDAL-3 Incore Monitoring System. Fewer detectors can still identify any significant anomalous condition, and PIDAL-3 can accurately monitor the peaking factors.

Figure 1 Cycle 14 Relative Assembly Powers at Detector Locations with Dropped Control Rod

Detector	ARO	A-07	A-08	A-10	A-12	B-18	B-20	1-26	1-28	2-32	3-35	3-36	3-37	4-41
1	0.292	0.306	0.312	0.297	0.297	0.316	0.318	0.308	0.310	0.315	0.307	0.306	0.310	0.312
2	0.645	0.681	0.687	0.655	0.655	0.700	0.701	0.681	0.684	0.695	0.677	0.680	0.684	0.689
3	1.111	1.154	1.182	1.126	1.127	1.194	1.203	1.165	1.176	1.190	1.164	1.155	1.177	1.182
4	1.409	1.470	1.495	1.429	1.430	1.519	1.525	1.481	1.490	1.509	1.466	1.476	1.490	1.499
5	1.420	1.459	1.506	1.438	1.440	1.513	1.531	1.480	1.499	1.511	1.481	1.459	1.501	1.504
6	0.703	0.745	0.745	0.713	0.713	0.764	0.762	0.743	0.744	0.757	0.734	0.743	0.743	0.750
7	0.703	0.710	0.744	0.710	0.712	0.733	0.755	0.719	0.741	0.740	0.734	0.688	0.743	0.739
8	0.874	0.928	0.924	0.887	0.887	0.950	0.947	0.923	0.924	0.941	0.914	0.925	0.923	0.932
9	1.145	1.207	1.207	1.162	1.162	1.240	1.238	1.208	1.210	1.228	1.183	1.209	1.209	1.220
10	1.118	1.158	1.173	1.134	1.135	1.205	1.207	1.177	1.181	1.192	1.127	1.175	1.181	1.189
11	1.145	1.138	1.207	1.156	1.160	1.189	1.226	1.171	1.205	1.199	1.183	1.126	1.209	1.201
12	0.877	0.877	0.927	0.883	0.887	0.891	0.936	0.877	0.922	0.914	0.917	0.803	0.926	0.913
13	0.197	0.210	0.208	0.200	0.200	0.215	0.214	0.208	0.208	0.213	0.207	0.209	0.208	0.211
14	1.106	1.101	1.137	1.120	1.120	1.179	1.185	1.157	1.164	1.158	1.040	1.153	1.164	1.169
15	1.481	1.394	1.529	1.496	1.499	1.545	1.577	1.528	1.555	1.528	1.433	1.505	1.558	1.553
16	1.498	1.441	1.567	1.510	1.516	1.523	1.592	1.512	1.572	1.544	1.530	1.435	1.578	1.559
17	1.111	1.182	1.170	1.128	1.127	1.208	1.202	1.175	1.174	1.195	1.164	1.177	1.169	1.185
18	1.543	1.629	1.612	1.565	1.565	1.669	1.662	1.627	1.625	1.649	1.589	1.629	1.620	1.640
19	1.280	1.290	1.292	1.297	1.297	1.368	1.366	1.342	1.344	1.336	1.157	1.341	1.342	1.353
20	1.230	1.208	1.290	1.230	1.242	1.181	1.293	1.166	1.285	1.254	1.280	0.951	1.292	1.253
21	1.497	0.875	1.447	1.507	1.511	1.493	1.545	1.521	1.552	1.415	1.256	1.507	1.559	1.535
22	1.106	0.655	1.101	1.108	1.115	1.054	1.137	1.096	1.145	1.038	1.040	1.072	1.153	1.120
23	0.890	0.948	0.930	0.903	0.903	0.967	0.959	0.941	0.937	0.955	0.932	0.943	0.930	0.948
24	1.308	1.369	1.319	1.326	1.325	1.409	1.392	1.377	1.368	1.380	1.306	1.381	1.357	1.384
25	1.106	1.137	1.070	1.120	1.119	1.183	1.166	1.161	1.152	1.147	1.040	1.164	1.142	1.165
26	1.497	1.495	1.363	1.515	1.514	1.584	1.560	1.564	1.552	1.513	1.256	1.568	1.541	1.566
27	1.299	1.099	1.091	1.309	1.309	1.310	1.310	1.331	1.332	1.172	0.749	1.333	1.334	1.327
28	1.161	1.131	1.205	1.135	1.165	0.931	1.179	0.894	1.195	1.132	1.208	0.624	1.211	1.109
29	1.280	1.097	1.075	1.280	1.280	1.191	1.194	1.278	1.278	0.721	1.157	1.293	1.293	1.246
30	1.111	1.104	1.155	1.054	1.111	0.851	1.110	0.484	1.134	1.082	1.164	0.803	1.155	1.011
31	1.481	1.516	1.275	1.497	1.490	1.558	1.484	1.544	1.493	1.478	1.433	1.553	1.451	1.529
32	1.106	1.070	0.655	1.110	1.103	1.093	0.985	1.128	1.076	0.910	1.040	1.142	1.072	1.087
33	1.135	1.074	1.069	1.119	1.120	0.907	0.916	1.086	1.087	0.640	1.132	1.129	1.127	0.986
34	0.352	0.376	0.364	0.358	0.357	0.383	0.377	0.373	0.369	0.377	0.370	0.374	0.362	0.375
35	1.145	1.207	1.140	1.160	1.156	1.227	1.188	1.203	1.171	1.198	1.183	1.209	1.129	1.201
36	1.145	1.140	1.138	1.099	1.100	0.865	0.871	1.043	1.041	0.995	1.183	1.129	1.125	0.609
37	1.439	1.518	1.437	1.457	1.451	1.538	1.477	1.510	1.455	1.502	1.496	1.517	1.377	1.503
38	1.305	1.372	1.281	1.320	1.312	1.387	1.311	1.366	1.297	1.347	1.351	1.374	1.201	1.352
39	1.267	1.303	1.189	1.270	1.245	1.275	0.987	1.298	1.073	1.201	1.300	1.318	1.014	1.212
40	0.703	0.711	0.710	0.642	0.642	0.556	0.559	0.619	0.617	0.647	0.734	0.691	0.688	0.303
41	0.140	0.141	0.144	0.072	0.136	0.101	0.128	0.097	0.135	0.132	0.147	0.130	0.143	0.095
42	0.369	0.391	0.372	0.373	0.372	0.396	0.380	0.388	0.373	0.387	0.386	0.390	0.351	0.387
43	1.111	1.170	1.104	1.122	1.109	1.171	1.063	1.160	1.030	1.138	1.164	1.170	0.802	1.131
44	0.645	0.669	0.643	0.641	0.576	0.629	0.470	0.650	0.254	0.622	0.677	0.668	0.526	0.548
45	0.327	0.342	0.326	0.327	0.310	0.329	0.258	0.335	0.169	0.322	0.344	0.341	0.224	0.301

Quadrant Power Tilt Fractions

Quadrant	ARO	A-07	A-08	A-10	A-12	B-18	B-20	1-26	1-28	2-32	3-35	3-36	3-37	4-41
1	1.000	0.956	1.041	1.007	1.012	1.018	1.062	1.007	1.049	1.030	1.000	0.945	1.053	1.040
2	1.000	1.041	1.042	1.014	1.014	1.079	1.077	1.053	1.055	1.065	1.000	1.053	1.053	1.063
3	1.000	1.042	0.961	1.012	1.007	1.064	1.018	1.047	1.007	1.030	1.000	1.053	0.950	1.041
4	1.000	0.961	0.956	0.967	0.967	0.839	0.843	0.893	0.889	0.876	1.000	0.950	0.944	0.856

Figure 2 Cycle 14 Percent Deviations in Relative Assembly Powers from ARO with Dropped CR

Detector	ARO	A-07	A-08	A-10	A-12	B-18	B-20	1-26	1-28	2-32	3-35	3-36	3-37	4-41
1	0.0	4.8	6.8	1.7	1.7	8.2	8.9	5.5	6.2	7.9	5.1	4.8	6.2	6.8
2	0.0	5.6	6.5	1.6	1.6	8.5	8.7	5.6	6.0	7.8	5.0	5.4	6.0	6.8
3	0.0	3.9	6.4	1.4	1.4	7.5	8.3	4.9	5.9	7.1	4.8	4.0	5.9	6.4
4	0.0	4.3	6.1	1.4	1.5	7.8	8.2	5.1	5.7	7.1	4.0	4.8	5.7	6.4
5	0.0	1.2	1.3	1.2	1.2	1.3	1.3	1.2	1.3	1.3	1.2	1.2	1.3	1.3
6	0.0	6.0	6.0	1.4	1.4	8.7	8.4	5.7	5.8	7.7	4.4	5.7	5.7	6.7
7	0.0	1.0	5.8	1.0	1.3	4.3	7.4	2.3	5.4	5.3	4.4	-2.1	5.7	5.1
8	0.0	6.2	5.7	1.5	1.5	8.7	8.4	5.6	5.7	7.7	4.6	5.8	5.6	6.6
9	0.0	5.4	5.4	1.5	1.5	8.3	8.1	5.5	5.7	7.2	3.3	5.6	5.6	6.6
10	0.0	3.6	4.9	1.4	1.5	7.8	8.0	5.3	5.6	6.6	0.8	5.1	5.6	6.4
11	0.0	-0.6	5.4	1.0	1.3	3.8	7.1	2.3	5.2	4.7	3.3	-1.7	5.6	4.9
12	0.0	0.0	5.7	0.7	1.1	1.6	6.7	0.0	5.1	4.2	4.6	-8.4	5.6	4.1
13	0.0	6.6	5.6	1.5	1.5	9.1	8.6	5.6	5.6	8.1	5.1	6.1	5.6	7.1
14	0.0	-0.5	2.8	1.3	1.3	6.6	7.1	4.6	5.2	4.7	-6.0	4.2	5.2	5.7
15	0.0	-5.9	3.2	1.0	1.2	4.3	6.5	3.2	5.0	3.2	-3.2	1.6	5.2	4.9
16	0.0	-3.8	4.6	0.8	1.2	1.7	6.3	0.9	4.9	3.1	2.1	-4.2	5.3	4.1
17	0.0	6.4	5.3	1.5	1.4	8.7	8.2	5.8	5.7	7.6	4.8	5.9	5.2	6.7
18	0.0	5.6	4.5	1.4	1.4	8.2	7.7	5.4	5.3	6.9	3.0	5.6	5.0	6.3
19	0.0	0.8	0.9	1.3	1.3	6.9	6.7	4.8	5.0	4.4	-9.6	4.8	4.8	5.7
20	0.0	-1.8	4.9	0.0	1.0	-4.0	5.1	-5.2	4.5	2.0	4.1	-22.7	5.0	1.9
21	0.0	-41.5	-3.3	0.7	0.9	-0.3	3.2	1.6	3.7	-5.5	-16.1	0.7	4.1	2.5
22	0.0	-40.8	-0.5	0.2	0.8	-4.7	2.8	-0.9	3.5	-6.1	-6.0	-3.1	4.2	1.3
23	0.0	6.5	4.5	1.5	1.5	8.7	7.8	5.7	5.3	7.3	4.7	6.0	4.5	6.5
24	0.0	4.7	0.8	1.4	1.3	7.7	6.4	5.3	4.6	5.5	-0.2	5.6	3.7	5.8
25	0.0	2.8	-3.3	1.3	1.2	7.0	5.4	5.0	4.2	3.7	-6.0	5.2	3.3	5.3
26	0.0	-0.1	-9.0	1.2	1.1	5.8	4.2	4.5	3.7	1.1	-16.1	4.7	2.9	4.6
27	0.0	-15.4	-16.0	0.8	0.8	0.8	0.8	2.5	2.5	-9.8	-42.3	2.6	2.7	2.2
28	0.0	-2.6	3.8	-2.2	0.3	-19.8	1.6	-23.0	2.9	-2.5	4.0	-46.3	4.3	-4.5
29	0.0	-14.3	-16.0	0.0	0.0	-7.0	-6.7	-0.2	-0.2	-43.7	-9.6	1.0	1.0	-2.7
30	0.0	-0.6	4.0	-5.1	0.0	-23.4	-0.1	-56.4	2.1	-2.6	4.8	-27.7	4.0	-9.0
31	0.0	2.4	-13.9	1.1	0.6	5.2	0.2	4.3	0.8	-0.2	-3.2	4.9	-2.0	3.2
32	0.0	-3.3	-40.8	0.4	-0.3	-1.2	-10.9	2.0	-2.7	-17.7	-6.0	3.3	-3.1	-1.7
33	0.0	-5.4	-5.8	-1.4	-1.3	-20.1	-19.3	-4.3	-4.2	-43.6	-0.3	-0.5	-0.7	-13.1
34	0.0	6.8	3.4	1.7	1.4	8.8	7.1	6.0	4.8	7.1	5.1	6.3	2.8	6.5
35	0.0	5.4	-0.4	1.3	1.0	7.2	3.8	5.1	2.3	4.6	3.3	5.6	-1.4	4.9
36	0.0	-0.4	-0.6	-4.0	-3.9	-24.5	-23.9	-8.9	-9.1	-13.1	3.3	-1.4	-1.7	-46.8
37	0.0	5.5	-0.1	1.3	0.8	6.9	2.6	4.9	1.1	4.4	4.0	5.4	-4.3	4.4
38	0.0	5.1	-1.8	1.1	0.5	6.3	0.5	4.7	-0.6	3.2	3.5	5.3	-8.0	3.6
39	0.0	2.8	-6.2	0.2	-1.7	0.6	-22.1	2.4	-15.3	-5.2	2.6	4.0	-20.0	-4.3
40	0.0	1.1	1.0	-8.7	-8.7	-20.9	-20.5	-11.9	-12.2	-8.0	4.4	-1.7	-2.1	-56.9
41	0.0	0.7	2.9	-48.6	-2.9	-27.9	-8.6	-30.7	-3.6	-5.7	5.0	-7.1	2.1	-32.1
42	0.0	6.0	0.8	1.1	0.8	7.3	3.0	5.1	1.1	4.9	4.6	5.7	-4.9	4.9
43	0.0	5.3	-0.6	1.0	-0.2	5.4	-4.3	4.4	-7.3	2.4	4.8	5.3	-27.8	1.8
44	0.0	3.7	-0.3	-0.6	-10.7	-2.5	-27.1	0.8	-60.6	-3.6	5.0	3.6	-18.4	-15.0
45	0.0	4.6	-0.3	0.0	-5.2	0.6	-21.1	2.4	-48.3	-1.5	5.2	4.3	-31.5	-8.0

Quadrant Power Tilt Fractions														
Quadrant	ARO	A-07	A-08	A-10	A-12	B-18	B-20	1-26	1-28	2-32	3-35	3-36	3-37	4-41
1	1.000	0.956	1.041	1.007	1.012	1.018	1.062	1.007	1.049	1.030	1.000	0.945	1.053	1.040
2	1.000	1.041	1.042	1.014	1.014	1.079	1.077	1.053	1.055	1.065	1.000	1.053	1.053	1.063
3	1.000	1.042	0.961	1.012	1.007	1.064	1.018	1.047	1.007	1.030	1.000	1.053	0.950	1.041
4	1.000	0.961	0.956	0.967	0.967	0.839	0.843	0.893	0.889	0.876	1.000	0.950	0.944	0.856

Figure 3 Cycle 14 Relative Assembly Powers at Detector Locations with CR at 120 Inches

Detector	ARO	A-07	A-08	A-10	A-12	B-18	B-20	1-26	1-28	2-32	3-35	3-36	3-37	4-41
1	0.292	0.293	0.293	0.292	0.292	0.293	0.293	0.293	0.293	0.293	0.293	0.293	0.293	0.293
2	0.645	0.647	0.647	0.646	0.646	0.648	0.648	0.647	0.647	0.648	0.646	0.647	0.647	0.647
3	1.111	1.113	1.115	1.112	1.112	1.115	1.116	1.114	1.114	1.115	1.114	1.113	1.114	1.114
4	1.409	1.412	1.414	1.410	1.410	1.415	1.415	1.413	1.413	1.414	1.412	1.413	1.413	1.414
5	1.420	1.422	1.425	1.421	1.421	1.425	1.426	1.423	1.424	1.425	1.423	1.422	1.424	1.424
6	0.703	0.705	0.705	0.703	0.703	0.706	0.706	0.705	0.705	0.706	0.704	0.704	0.704	0.705
7	0.703	0.703	0.705	0.703	0.703	0.704	0.705	0.703	0.704	0.705	0.704	0.702	0.705	0.704
8	0.874	0.877	0.877	0.874	0.874	0.877	0.877	0.876	0.876	0.877	0.876	0.876	0.876	0.877
9	1.145	1.148	1.149	1.146	1.146	1.150	1.150	1.148	1.148	1.150	1.147	1.148	1.148	1.149
10	1.118	1.121	1.121	1.119	1.119	1.123	1.123	1.121	1.122	1.122	1.119	1.121	1.122	1.122
11	1.145	1.145	1.148	1.146	1.146	1.148	1.149	1.146	1.148	1.148	1.147	1.145	1.148	1.148
12	0.877	0.877	0.879	0.877	0.877	0.878	0.880	0.877	0.879	0.879	0.879	0.874	0.879	0.879
13	0.197	0.197	0.197	0.197	0.197	0.198	0.198	0.197	0.197	0.198	0.197	0.197	0.197	0.197
14	1.106	1.105	1.107	1.106	1.106	1.109	1.109	1.108	1.108	1.108	1.102	1.108	1.108	1.109
15	1.481	1.477	1.483	1.482	1.482	1.484	1.486	1.483	1.484	1.484	1.479	1.482	1.484	1.484
16	1.498	1.496	1.503	1.499	1.499	1.500	1.503	1.500	1.502	1.501	1.501	1.496	1.502	1.502
17	1.111	1.115	1.114	1.112	1.112	1.116	1.115	1.114	1.114	1.115	1.114	1.114	1.114	1.115
18	1.543	1.548	1.547	1.544	1.544	1.549	1.549	1.547	1.547	1.549	1.545	1.547	1.547	1.548
19	1.280	1.281	1.281	1.281	1.281	1.285	1.285	1.283	1.283	1.283	1.275	1.283	1.283	1.284
20	1.230	1.229	1.233	1.229	1.230	1.228	1.233	1.227	1.232	1.231	1.232	1.216	1.233	1.231
21	1.497	1.460	1.496	1.499	1.499	1.498	1.500	1.499	1.501	1.494	1.487	1.499	1.501	1.500
22	1.106	1.076	1.105	1.106	1.106	1.103	1.107	1.105	1.108	1.102	1.102	1.104	1.108	1.106
23	0.890	0.893	0.892	0.891	0.891	0.894	0.894	0.893	0.892	0.893	0.892	0.892	0.892	0.893
24	1.308	1.311	1.309	1.309	1.309	1.313	1.312	1.311	1.311	1.312	1.308	1.311	1.311	1.312
25	1.106	1.107	1.104	1.106	1.106	1.109	1.108	1.108	1.108	1.108	1.102	1.108	1.108	1.108
26	1.497	1.498	1.491	1.499	1.499	1.502	1.501	1.501	1.501	1.499	1.487	1.501	1.500	1.501
27	1.299	1.289	1.289	1.300	1.300	1.299	1.300	1.301	1.301	1.293	1.267	1.301	1.301	1.301
28	1.161	1.160	1.164	1.160	1.162	1.151	1.162	1.149	1.163	1.160	1.164	1.131	1.164	1.160
29	1.280	1.271	1.270	1.281	1.280	1.276	1.276	1.280	1.281	1.246	1.275	1.281	1.281	1.279
30	1.111	1.111	1.113	1.109	1.111	1.100	1.111	1.077	1.112	1.110	1.114	1.097	1.113	1.107
31	1.481	1.483	1.470	1.482	1.482	1.485	1.481	1.484	1.482	1.481	1.479	1.484	1.480	1.483
32	1.106	1.104	1.076	1.106	1.105	1.105	1.099	1.107	1.104	1.095	1.102	1.107	1.104	1.105
33	1.135	1.132	1.132	1.135	1.135	1.123	1.124	1.133	1.133	1.102	1.135	1.135	1.135	1.128
34	0.352	0.354	0.353	0.353	0.353	0.354	0.354	0.353	0.353	0.354	0.353	0.354	0.353	0.354
35	1.145	1.148	1.145	1.146	1.146	1.149	1.148	1.148	1.147	1.148	1.147	1.148	1.145	1.148
36	1.145	1.145	1.145	1.143	1.143	1.131	1.131	1.141	1.141	1.137	1.147	1.145	1.145	1.112
37	1.439	1.443	1.439	1.440	1.440	1.444	1.441	1.442	1.440	1.442	1.441	1.443	1.437	1.442
38	1.305	1.309	1.304	1.306	1.306	1.309	1.306	1.308	1.305	1.308	1.307	1.308	1.301	1.308
39	1.267	1.269	1.263	1.267	1.266	1.267	1.253	1.268	1.258	1.263	1.268	1.269	1.255	1.264
40	0.703	0.703	0.703	0.700	0.700	0.696	0.696	0.699	0.699	0.700	0.704	0.702	0.702	0.678
41	0.140	0.140	0.140	0.135	0.140	0.139	0.140	0.138	0.140	0.140	0.141	0.140	0.140	0.138
42	0.369	0.370	0.369	0.369	0.369	0.370	0.369	0.370	0.369	0.370	0.369	0.370	0.368	0.369
43	1.111	1.114	1.111	1.112	1.111	1.114	1.109	1.114	1.108	1.113	1.114	1.114	1.097	1.112
44	0.645	0.646	0.645	0.645	0.642	0.644	0.637	0.645	0.621	0.644	0.646	0.646	0.640	0.641
45	0.327	0.328	0.327	0.327	0.326	0.327	0.324	0.327	0.319	0.327	0.328	0.328	0.322	0.326

Quadrant Power Tilt Fractions														
Quadrant	ARO	A-07	A-08	A-10	A-12	B-18	B-20	1-26	1-28	2-32	3-35	3-36	3-37	4-41
1	1.000	0.998	1.002	1.000	1.001	1.001	1.003	1.000	1.002	1.002	1.000	0.997	1.003	1.002
2	1.000	1.002	1.002	1.001	1.001	1.004	1.004	1.003	1.003	1.003	1.000	1.003	1.003	1.003
3	1.000	1.002	0.998	1.001	1.000	1.003	1.001	1.002	1.001	1.002	1.000	1.003	0.998	1.002
4	1.000	0.998	0.998	0.998	0.998	0.992	0.992	0.995	0.995	0.993	1.000	0.998	0.997	0.993

Figure 4 Cycle 14 Percent Deviations in Relative Assembly Powers from ARO with CR at 120 Inches

Detector	ARO	A-07	A-08	A-10	A-12	B-18	B-20	1-26	1-28	2-32	3-35	3-36	3-37	4-41
1	0.0	0.3	0.3	0.0	0.0	0.3	0.3	0.3	0.3	0.3	0.3	0.3	0.3	0.3
2	0.0	0.3	0.3	0.2	0.2	0.5	0.5	0.3	0.3	0.5	0.2	0.3	0.3	0.3
3	0.0	0.2	0.4	0.1	0.1	0.4	0.5	0.3	0.3	0.4	0.3	0.2	0.3	0.3
4	0.0	0.2	0.4	0.1	0.1	0.4	0.4	0.3	0.3	0.4	0.2	0.3	0.3	0.4
5	0.0	1.2	1.3	1.2	1.2	1.3	1.3	1.2	1.3	1.3	1.2	1.2	1.3	1.3
6	0.0	0.3	0.3	0.0	0.0	0.4	0.4	0.3	0.3	0.4	0.1	0.1	0.1	0.3
7	0.0	0.0	0.3	0.0	0.0	0.1	0.3	0.0	0.1	0.3	0.1	-0.1	0.3	0.1
8	0.0	0.3	0.3	0.0	0.0	0.3	0.3	0.2	0.2	0.3	0.2	0.2	0.2	0.3
9	0.0	0.3	0.3	0.1	0.1	0.4	0.4	0.3	0.3	0.4	0.2	0.3	0.3	0.3
10	0.0	0.3	0.3	0.1	0.1	0.4	0.4	0.3	0.4	0.4	0.1	0.3	0.4	0.4
11	0.0	0.0	0.3	0.1	0.1	0.3	0.3	0.1	0.3	0.3	0.2	0.0	0.3	0.3
12	0.0	0.0	0.2	0.0	0.0	0.1	0.3	0.0	0.2	0.2	0.2	-0.3	0.2	0.2
13	0.0	0.0	0.0	0.0	0.0	0.5	0.5	0.0	0.0	0.5	0.0	0.0	0.0	0.0
14	0.0	-0.1	0.1	0.0	0.0	0.3	0.3	0.2	0.2	0.2	-0.4	0.2	0.2	0.3
15	0.0	-0.3	0.1	0.1	0.1	0.2	0.3	0.1	0.2	0.2	-0.1	0.1	0.2	0.2
16	0.0	-0.1	0.3	0.1	0.1	0.1	0.3	0.1	0.3	0.2	0.2	-0.1	0.3	0.3
17	0.0	0.4	0.3	0.1	0.1	0.5	0.4	0.3	0.3	0.4	0.3	0.3	0.3	0.4
18	0.0	0.3	0.3	0.1	0.1	0.4	0.4	0.3	0.3	0.4	0.1	0.3	0.3	0.3
19	0.0	0.1	0.1	0.1	0.1	0.4	0.4	0.2	0.2	0.2	-0.4	0.2	0.2	0.3
20	0.0	-0.1	0.2	-0.1	0.0	-0.2	0.2	-0.2	0.2	0.1	0.2	-1.1	0.2	0.1
21	0.0	-2.5	-0.1	0.1	0.1	0.1	0.2	0.1	0.3	-0.2	-0.7	0.1	0.3	0.2
22	0.0	-2.7	-0.1	0.0	0.0	-0.3	0.1	-0.1	0.2	-0.4	-0.4	-0.2	0.2	0.0
23	0.0	0.3	0.2	0.1	0.1	0.4	0.4	0.3	0.2	0.3	0.2	0.2	0.2	0.3
24	0.0	0.2	0.1	0.1	0.1	0.4	0.3	0.2	0.2	0.3	0.0	0.2	0.2	0.3
25	0.0	0.1	-0.2	0.0	0.0	0.3	0.2	0.2	0.2	0.2	-0.4	0.2	0.2	0.2
26	0.0	0.1	-0.4	0.1	0.1	0.3	0.3	0.3	0.3	0.1	-0.7	0.3	0.2	0.3
27	0.0	-0.8	-0.8	0.1	0.1	0.0	0.1	0.2	0.2	-0.5	-2.5	0.2	0.2	0.2
28	0.0	-0.1	0.3	-0.1	0.1	-0.9	0.1	-1.0	0.2	-0.1	0.3	-2.6	0.3	-0.1
29	0.0	-0.7	-0.8	0.1	0.0	-0.3	-0.3	0.0	0.1	-2.7	-0.4	0.1	0.1	-0.1
30	0.0	0.0	0.2	-0.2	0.0	-1.0	0.0	-3.1	0.1	-0.1	0.3	-1.3	0.2	-0.4
31	0.0	0.1	-0.7	0.1	0.1	0.3	0.0	0.2	0.1	0.0	-0.1	0.2	-0.1	0.1
32	0.0	-0.2	-2.7	0.0	-0.1	-0.1	-0.6	0.1	-0.2	-1.0	-0.4	0.1	-0.2	-0.1
33	0.0	-0.3	-0.3	0.0	0.0	-1.1	-1.0	-0.2	-0.2	-2.9	0.0	0.0	0.0	-0.6
34	0.0	0.6	0.3	0.3	0.3	0.6	0.6	0.3	0.3	0.6	0.3	0.6	0.3	0.6
35	0.0	0.3	0.0	0.1	0.1	0.3	0.3	0.3	0.2	0.3	0.2	0.3	0.0	0.3
36	0.0	0.0	0.0	-0.2	-0.2	-1.2	-1.2	-0.3	-0.3	-0.7	0.2	0.0	0.0	-2.9
37	0.0	0.3	0.0	0.1	0.1	0.3	0.1	0.2	0.1	0.2	0.1	0.3	-0.1	0.2
38	0.0	0.3	-0.1	0.1	0.1	0.3	0.1	0.2	0.0	0.2	0.2	0.2	-0.3	0.2
39	0.0	0.2	-0.3	0.0	-0.1	0.0	-1.1	0.1	-0.7	-0.3	0.1	0.2	-0.9	-0.2
40	0.0	0.0	0.0	-0.4	-0.4	-1.0	-1.0	-0.6	-0.6	-0.4	0.1	-0.1	-0.1	-3.6
41	0.0	0.0	0.0	-3.6	0.0	-0.7	0.0	-1.4	0.0	0.0	0.7	0.0	0.0	-1.4
42	0.0	0.3	0.0	0.0	0.0	0.3	0.0	0.3	0.0	0.3	0.0	0.3	-0.3	0.0
43	0.0	0.3	0.0	0.1	0.0	0.3	-0.2	0.3	-0.3	0.2	0.3	0.3	-1.3	0.1
44	0.0	0.2	0.0	0.0	-0.5	-0.2	-1.2	0.0	-3.7	-0.2	0.2	0.2	-0.8	-0.6
45	0.0	0.3	0.0	0.0	-0.3	0.0	-0.9	0.0	-2.4	0.0	0.3	0.3	-1.5	-0.3

Quadrant Power Tilt Fractions

Quadrant	ARO	A-07	A-08	A-10	A-12	B-18	B-20	1-26	1-28	2-32	3-35	3-36	3-37	4-41
1	1.000	0.998	1.002	1.000	1.001	1.001	1.003	1.000	1.002	1.002	1.000	0.997	1.003	1.002
2	1.000	1.002	1.002	1.001	1.001	1.004	1.004	1.003	1.003	1.003	1.000	1.003	1.003	1.003
3	1.000	1.002	0.998	1.001	1.000	1.003	1.001	1.002	1.001	1.002	1.000	1.003	0.998	1.002
4	1.000	0.998	0.998	0.998	0.998	0.992	0.992	0.995	0.995	0.993	1.000	0.998	0.997	0.993

Figure 5 Cycle 14 Relative Assembly Powers at Detector Locations with CR 4-41 Mis-Aligned

Detector	PDIL	+4 IN	-4 IN	+8 IN	-8 IN	+16 IN	-16IN
1	0.298	0.297	0.298	0.297	0.298	0.295	0.300
2	0.645	0.645	0.645	0.645	0.645	0.639	0.652
3	1.125	1.124	1.126	1.124	1.126	1.115	1.136
4	1.433	1.432	1.434	1.431	1.435	1.420	1.447
5	1.410	1.410	1.410	1.411	1.409	1.398	1.423
6	0.640	0.642	0.637	0.644	0.634	0.633	0.647
7	0.640	0.642	0.637	0.644	0.634	0.635	0.645
8	0.846	0.847	0.845	0.848	0.844	0.838	0.854
9	1.070	1.073	1.067	1.075	1.063	1.060	1.081
10	1.129	1.128	1.129	1.128	1.130	1.118	1.139
11	1.070	1.073	1.067	1.075	1.063	1.063	1.078
12	0.849	0.850	0.848	0.851	0.847	0.845	0.855
13	0.198	0.198	0.198	0.198	0.198	0.196	0.200
14	1.131	1.130	1.132	1.130	1.134	1.122	1.141
15	1.506	1.505	1.507	1.504	1.509	1.496	1.517
16	1.483	1.484	1.482	1.484	1.482	1.475	1.492
17	1.125	1.124	1.126	1.124	1.126	1.114	1.136
18	1.555	1.554	1.555	1.554	1.556	1.541	1.569
19	1.311	1.310	1.313	1.309	1.314	1.301	1.322
20	1.240	1.240	1.241	1.240	1.242	1.238	1.244
21	1.540	1.538	1.542	1.537	1.544	1.535	1.546
22	1.131	1.130	1.133	1.130	1.134	1.130	1.134
23	0.906	0.905	0.907	0.905	0.908	0.898	0.915
24	1.333	1.332	1.334	1.331	1.335	1.322	1.345
25	1.131	1.130	1.133	1.130	1.134	1.123	1.140
26	1.540	1.538	1.542	1.537	1.544	1.530	1.550
27	1.339	1.337	1.341	1.336	1.342	1.336	1.343
28	1.181	1.180	1.181	1.179	1.182	1.190	1.173
29	1.311	1.310	1.313	1.309	1.314	1.317	1.306
30	1.125	1.124	1.126	1.124	1.126	1.141	1.110
31	1.506	1.505	1.507	1.504	1.509	1.500	1.513
32	1.131	1.130	1.132	1.130	1.134	1.135	1.129
33	1.139	1.139	1.140	1.139	1.140	1.161	1.118
34	0.346	0.347	0.346	0.347	0.346	0.343	0.350
35	1.070	1.073	1.067	1.075	1.063	1.063	1.078
36	1.070	1.073	1.067	1.075	1.063	1.132	0.985
37	1.341	1.345	1.337	1.348	1.331	1.333	1.350
38	1.286	1.286	1.285	1.287	1.284	1.280	1.292
39	1.288	1.287	1.289	1.286	1.289	1.297	1.279
40	0.640	0.642	0.637	0.644	0.634	0.688	0.578
41	0.135	0.136	0.135	0.136	0.135	0.142	0.129
42	0.348	0.349	0.347	0.350	0.347	0.346	0.351
43	1.125	1.124	1.126	1.124	1.126	1.123	1.127
44	0.645	0.645	0.645	0.645	0.645	0.660	0.631
45	0.332	0.332	0.332	0.331	0.332	0.336	0.328

Quadrant Power Tilt Fractions							
Quadrant	PDIL	+4 IN	-4 IN	+8 IN	-8 IN	+16 IN	-16IN
1	1.000	1.000	1.000	1.000	1.000	0.995	1.006
2	1.000	1.000	1.000	1.000	1.000	0.991	1.009
3	1.000	1.000	1.000	1.000	1.000	0.995	1.006
4	1.000	1.000	1.000	1.000	1.000	1.020	0.979

Figure 6 Cycle 14 Percent Deviations in Relative Asm. Powers from PDIL with CR 4-41 Mis-Aligned

Detector	PDIL	+4 IN	-4 IN	+8 IN	-8 IN	+16 IN	-16IN
1	0.0	-0.3	0.0	-0.3	0.0	-1.0	0.7
2	0.0	0.0	0.0	0.0	0.0	-0.9	1.1
3	0.0	-0.1	0.1	-0.1	0.1	-0.9	1.0
4	0.0	-0.1	0.1	-0.1	0.1	-0.9	1.0
5	0.0	1.2	1.3	1.2	1.2	1.3	1.3
6	0.0	0.3	-0.5	0.6	-0.9	-1.1	1.1
7	0.0	0.3	-0.5	0.6	-0.9	-0.8	0.8
8	0.0	0.1	-0.1	0.2	-0.2	-0.9	0.9
9	0.0	0.3	-0.3	0.5	-0.7	-0.9	1.0
10	0.0	-0.1	0.0	-0.1	0.1	-1.0	0.9
11	0.0	0.3	-0.3	0.5	-0.7	-0.7	0.7
12	0.0	0.1	-0.1	0.2	-0.2	-0.5	0.7
13	0.0	0.0	0.0	0.0	0.0	-1.0	1.0
14	0.0	-0.1	0.1	-0.1	0.3	-0.8	0.9
15	0.0	-0.1	0.1	-0.1	0.2	-0.7	0.7
16	0.0	0.1	-0.1	0.1	-0.1	-0.5	0.6
17	0.0	-0.1	0.1	-0.1	0.1	-1.0	1.0
18	0.0	-0.1	0.0	-0.1	0.1	-0.9	0.9
19	0.0	-0.1	0.2	-0.2	0.2	-0.8	0.8
20	0.0	0.0	0.1	0.0	0.2	-0.2	0.3
21	0.0	-0.1	0.1	-0.2	0.3	-0.3	0.4
22	0.0	-0.1	0.2	-0.1	0.3	-0.1	0.3
23	0.0	-0.1	0.1	-0.1	0.2	-0.9	1.0
24	0.0	-0.1	0.1	-0.2	0.2	-0.8	0.9
25	0.0	-0.1	0.2	-0.1	0.3	-0.7	0.8
26	0.0	-0.1	0.1	-0.2	0.3	-0.6	0.6
27	0.0	-0.1	0.1	-0.2	0.2	-0.2	0.3
28	0.0	-0.1	0.0	-0.2	0.1	0.8	-0.7
29	0.0	-0.1	0.2	-0.2	0.2	0.5	-0.4
30	0.0	-0.1	0.1	-0.1	0.1	1.4	-1.3
31	0.0	-0.1	0.1	-0.1	0.2	-0.4	0.5
32	0.0	-0.1	0.1	-0.1	0.3	0.4	-0.2
33	0.0	0.0	0.1	0.0	0.1	1.9	-1.8
34	0.0	0.3	0.0	0.3	0.0	-0.9	1.2
35	0.0	0.3	-0.3	0.5	-0.7	-0.7	0.7
36	0.0	0.3	-0.3	0.5	-0.7	5.8	-7.9
37	0.0	0.3	-0.3	0.5	-0.7	-0.6	0.7
38	0.0	0.0	-0.1	0.1	-0.2	-0.5	0.5
39	0.0	-0.1	0.1	-0.2	0.1	0.7	-0.7
40	0.0	0.3	-0.5	0.6	-0.9	7.5	-9.7
41	0.0	0.7	0.0	0.7	0.0	5.2	-4.4
42	0.0	0.3	-0.3	0.6	-0.3	-0.6	0.9
43	0.0	-0.1	0.1	-0.1	0.1	-0.2	0.2
44	0.0	0.0	0.0	0.0	0.0	2.3	-2.2
45	0.0	0.0	0.0	-0.3	0.0	1.2	-1.2

Quadrant Power Tilt Fractions							
Quadrant	PDIL	+4 IN	-4 IN	+8 IN	-8 IN	+16 IN	-16IN
1	1.000	1.000	1.000	1.000	1.000	0.995	1.006
2	1.000	1.000	1.000	1.000	1.000	0.991	1.009
3	1.000	1.000	1.000	1.000	1.000	0.995	1.006
4	1.000	1.000	1.000	1.000	1.000	1.020	0.979

Figure 7 Cycle 14 Relative Assembly Powers at Detector Locations with Assemblies Mis-loaded

Detector	Base	R-13	R-41	R-49	R-57	R-41 SB1	P-01 P-21	Q-13 Q33	R-05 R-29
1	0.281	0.280	0.280	0.281	0.280	0.268	0.281	0.281	0.274
2	0.633	0.633	0.632	0.633	0.633	0.604	0.633	0.633	0.617
3	1.184	1.184	1.183	1.183	1.184	1.133	1.183	1.183	1.155
4	1.417	1.418	1.417	1.416	1.418	1.357	1.416	1.416	1.386
5	1.477	1.478	1.478	1.476	1.478	1.419	1.477	1.476	1.446
6	0.671	0.671	0.670	0.671	0.671	0.641	0.671	0.671	0.655
7	0.671	0.670	0.671	0.670	0.670	0.647	0.671	0.671	0.658
8	0.864	0.864	0.863	0.864	0.864	0.827	0.863	0.864	0.845
9	1.131	1.133	1.132	1.131	1.133	1.084	1.130	1.131	1.109
10	1.095	1.097	1.096	1.095	1.097	1.053	1.095	1.095	1.082
11	1.131	1.132	1.133	1.130	1.133	1.094	1.131	1.131	1.115
12	0.863	0.862	0.863	0.862	0.863	0.836	0.863	0.863	0.848
13	0.184	0.184	0.184	0.184	0.184	0.176	0.184	0.184	0.180
14	1.095	1.097	1.097	1.096	1.097	1.065	1.095	1.093	1.105
15	1.406	1.408	1.409	1.405	1.409	1.373	1.406	1.403	1.416
16	1.427	1.429	1.431	1.426	1.430	1.391	1.428	1.426	1.417
17	1.184	1.184	1.182	1.183	1.184	1.133	1.183	1.183	1.158
18	1.532	1.535	1.533	1.531	1.534	1.472	1.531	1.532	1.508
19	1.284	1.286	1.286	1.285	1.286	1.255	1.283	1.283	1.311
20	1.280	1.277	1.281	1.277	1.280	1.252	1.280	1.280	1.264
21	1.495	1.496	1.501	1.494	1.497	1.522	1.497	1.482	1.605
22	1.095	1.095	1.100	1.094	1.096	1.110	1.098	1.094	1.143
23	0.901	0.900	0.899	0.900	0.900	0.865	0.900	0.901	0.883
24	1.338	1.340	1.338	1.339	1.340	1.301	1.336	1.339	1.343
25	1.095	1.097	1.096	1.096	1.097	1.078	1.093	1.096	1.129
26	1.495	1.498	1.496	1.497	1.497	1.497	1.492	1.499	1.604
27	1.394	1.395	1.400	1.395	1.394	1.463	1.394	1.341	1.666
28	1.218	1.211	1.220	1.214	1.217	1.214	1.220	1.220	1.209
29	1.284	1.284	1.294	1.281	1.283	1.504	1.295	1.324	1.536
30	1.184	1.175	1.185	1.178	1.182	1.181	1.185	1.186	1.169
31	1.406	1.409	1.403	1.409	1.408	1.433	1.399	1.404	1.488
32	1.095	1.097	1.089	1.100	1.093	1.286	1.078	1.097	1.296
33	1.082	1.080	1.090	1.075	1.079	1.273	1.111	1.091	1.139
34	0.322	0.322	0.321	0.323	0.322	0.311	0.322	0.323	0.317
35	1.131	1.133	1.130	1.132	1.134	1.110	1.129	1.131	1.122
36	1.131	1.131	1.135	1.123	1.127	1.208	1.134	1.135	1.118
37	1.456	1.458	1.454	1.458	1.460	1.433	1.454	1.456	1.434
38	1.337	1.339	1.334	1.339	1.341	1.329	1.334	1.337	1.319
39	1.310	1.312	1.300	1.321	1.299	1.391	1.311	1.312	1.272
40	0.671	0.674	0.671	0.668	0.667	0.699	0.672	0.673	0.650
41	0.121	0.120	0.121	0.120	0.120	0.123	0.121	0.121	0.119
42	0.334	0.333	0.333	0.334	0.334	0.327	0.334	0.334	0.327
43	1.184	1.184	1.179	1.187	1.196	1.185	1.182	1.184	1.125
44	0.633	0.634	0.630	0.639	0.626	0.656	0.634	0.634	0.507
45	0.314	0.314	0.312	0.317	0.314	0.322	0.314	0.314	0.224

Quadrant Power Tilt Fractions									
Quadrant	Base	R-13	R-41	R-49	R-57	R-41 SB1	P-01 P-21	Q-13 Q33	R-05 R-29
1	1.000	1.000	1.001	0.999	1.001	0.976	1.000	0.999	0.997
2	1.000	1.001	1.000	1.000	1.001	0.963	0.999	1.000	0.991
3	1.000	1.001	0.998	1.001	1.002	0.993	0.998	0.999	1.007
4	1.000	0.998	1.001	1.000	0.996	1.068	1.003	1.002	1.005

Figure 8 Cycle 14 Percent Deviations in Relative Asm. Powers from Base with Assemblies Mis-loaded

Detector	Base	R-13	R-41	R-49	R-57	R-41 SB1	P-01 P-21	Q-13 Q33	R-05 R-29
1	0.0	-0.4	-0.4	0.0	-0.4	-4.6	0.0	0.0	-2.5
2	0.0	0.0	-0.2	0.0	0.0	-4.6	0.0	0.0	-2.5
3	0.0	0.0	-0.1	-0.1	0.0	-4.3	-0.1	-0.1	-2.4
4	0.0	0.1	0.0	-0.1	0.1	-4.2	-0.1	-0.1	-2.2
5	0.0	1.2	1.2	1.2	1.2	1.2	1.2	1.2	1.2
6	0.0	0.0	-0.1	0.0	0.0	-4.5	0.0	0.0	-2.4
7	0.0	-0.1	0.0	-0.1	-0.1	-3.6	0.0	0.0	-1.9
8	0.0	0.0	-0.1	0.0	0.0	-4.3	-0.1	0.0	-2.2
9	0.0	0.2	0.1	0.0	0.2	-4.2	-0.1	0.0	-1.9
10	0.0	0.2	0.1	0.0	0.2	-3.8	0.0	0.0	-1.2
11	0.0	0.1	0.2	-0.1	0.2	-3.3	0.0	0.0	-1.4
12	0.0	-0.1	0.0	-0.1	0.0	-3.1	0.0	0.0	-1.7
13	0.0	0.0	0.0	0.0	0.0	-4.3	0.0	0.0	-2.2
14	0.0	0.2	0.2	0.1	0.2	-2.7	0.0	-0.2	0.9
15	0.0	0.1	0.2	-0.1	0.2	-2.3	0.0	-0.2	0.7
16	0.0	0.1	0.3	-0.1	0.2	-2.5	0.1	-0.1	-0.7
17	0.0	0.0	-0.2	-0.1	0.0	-4.3	-0.1	-0.1	-2.2
18	0.0	0.2	0.1	-0.1	0.1	-3.9	-0.1	0.0	-1.6
19	0.0	0.2	0.2	0.1	0.2	-2.3	-0.1	-0.1	2.1
20	0.0	-0.2	0.1	-0.2	0.0	-2.2	0.0	0.0	-1.3
21	0.0	0.1	0.4	-0.1	0.1	1.8	0.1	-0.9	7.4
22	0.0	0.0	0.5	-0.1	0.1	1.4	0.3	-0.1	4.4
23	0.0	-0.1	-0.2	-0.1	-0.1	-4.0	-0.1	0.0	-2.0
24	0.0	0.1	0.0	0.1	0.1	-2.8	-0.1	0.1	0.4
25	0.0	0.2	0.1	0.1	0.2	-1.6	-0.2	0.1	3.1
26	0.0	0.2	0.1	0.1	0.1	0.1	-0.2	0.3	7.3
27	0.0	0.1	0.4	0.1	0.0	4.9	0.0	-3.8	19.5
28	0.0	-0.6	0.2	-0.3	-0.1	-0.3	0.2	0.2	-0.7
29	0.0	0.0	0.8	-0.2	-0.1	17.1	0.9	3.1	19.6
30	0.0	-0.8	0.1	-0.5	-0.2	-0.3	0.1	0.2	-1.3
31	0.0	0.2	-0.2	0.2	0.1	1.9	-0.5	-0.1	5.8
32	0.0	0.2	-0.5	0.5	-0.2	17.4	-1.6	0.2	18.4
33	0.0	-0.2	0.7	-0.6	-0.3	17.7	2.7	0.8	5.3
34	0.0	0.0	-0.3	0.3	0.0	-3.4	0.0	0.3	-1.6
35	0.0	0.2	-0.1	0.1	0.3	-1.9	-0.2	0.0	-0.8
36	0.0	0.0	0.4	-0.7	-0.4	6.8	0.3	0.4	-1.1
37	0.0	0.1	-0.1	0.1	0.3	-1.6	-0.1	0.0	-1.5
38	0.0	0.1	-0.2	0.1	0.3	-0.6	-0.2	0.0	-1.3
39	0.0	0.2	-0.8	0.8	-0.8	6.2	0.1	0.2	-2.9
40	0.0	0.4	0.0	-0.4	-0.6	4.2	0.1	0.3	-3.1
41	0.0	-0.8	0.0	-0.8	-0.8	1.7	0.0	0.0	-1.7
42	0.0	-0.3	-0.3	0.0	0.0	-2.1	0.0	0.0	-2.1
43	0.0	0.0	-0.4	0.3	1.0	0.1	-0.2	0.0	-5.0
44	0.0	0.2	-0.5	0.9	-1.1	3.6	0.2	0.2	-19.9
45	0.0	0.0	-0.6	1.0	0.0	2.5	0.0	0.0	-28.7

Quadrant Power Tilt Fractions									
Quadrant	Base	R-13	R-41	R-49	R-57	R-41 SB1	P-01 P-21	Q-13 Q33	R-05 R-29
1	1.000	1.000	1.001	0.999	1.001	0.976	1.000	0.999	0.997
2	1.000	1.001	1.000	1.000	1.001	0.963	0.999	1.000	0.991
3	1.000	1.001	0.998	1.001	1.002	0.993	0.998	0.999	1.007
4	1.000	0.998	1.001	1.000	0.996	1.068	1.003	1.002	1.005

NRC Question No. 4

Section 1.0 (seventh paragraph, last sentence) of the report states that the uncertainties associated with cycles 12 thru 14 are bounded by the current Palisades Technical Specifications for PIDAL-3 with CASMO-3/SIMULATE-3. Please explain why this is true.

Response to Question No. 4

The current Palisades Technical Specification measurement uncertainties are based on the original PIDAL SER approved in April of 1992. The following Table shows a comparison of the measurement uncertainties for the three PIDAL submittals:

	Peak Assembly (F_R^A)	Peak Pin (F_R^I)	Peak LHGR (F_Q)
PIDAL 1992	0.0401	0.0455	0.0623
PIDAL 1996	0.0345	0.0454	0.0561
PIDAL 2000	0.0375	0.0400	0.0425

The PIDAL 1992 uncertainties are the current measurement uncertainties. These numbers can be extracted from Figure 4.5a "New" in the latest PIDAL-3 submittal. The PIDAL 1996 uncertainties were part of the first PIDAL-3 submittal approved in May of 1997. These numbers can be extracted from Figure 4.5b, "11 Xenon" in the latest PIDAL-3 submittal. The PIDAL 2000 uncertainties are given in the latest PIDAL-3 submittal. These numbers are based on Figure 4.5a, "11 Xenon", and have been rounded up to the nearest quarter percent. Both of the PIDAL-3 submittals have lower measurement uncertainties and therefore, are bounded by the present measurement uncertainties.

NRC Question No. 5

Section 1.2 (page 5) of the report states "If employing an implicit detector model...." Who decides whether an implicit or explicit model is to be used? What criteria are used for the selection? Is this a user input? What would be the consequences of using the wrong detector system model?

Response to Question No. 5

The designer when developing the CASMO cross section sets for each sub-batch fuel type selects an implicit or explicit detector model. The CASMO-3 cross sections used an explicit detector model at the time of development, since it required only a self-shielding factor correction, which is independent of fuel type. Since then, we have successfully developed a geometry factor correction for the explicit detector model, which is fuel type dependent. Naturally, this is more work, since it requires individual CASMO cases for each sub-batch fuel type, and it also introduces additional uncertainty with an additional correction.

The benefit of using an implicit detector model is that it models water in all of the assembly instrument tubes. This raises pin peaking around the instrument tube, and more accurately represents actual core configuration, since a maximum of 43 of 204 assemblies can be instrumented. Since the implicit model also adds slightly more reactivity to each assembly, it reduces our boron letdown anomaly between measurement and SIMULATE-3 by 10-20 PPM. The CASMO-4 cross-sections used in the benchmarking for this PIDAL-3 submittal used an implicit detector model. These two corrections are curve fitted and the coefficients are inputs to PIDAL-3. If the wrong model were utilized the results would be abnormally large deviations between measurements and SIMULATE-3, not unlike any other modeling error from CASMO-4 through PIDAL-3. All of this type of work is performed under Administrative Procedure 9.11 "Engineering Analysis" where it receives extensive technical and administrative reviews, and a 10 CFR 50.59 Safety Review. Palisades also has extensive administrative controls in place on software control with Administrative Procedure 9.14 "Control of Computer Software", and Software Quality Assurance Plans SQAP-029 and SQAP-050.

NRC Question No. 6

The first paragraph of Section 4.4.3 (page 26) of the report refers to "current ABBCE specifications." Please either provide references, summarize the pertinent elements of these specifications, or supply these specifications.

Response to Question No. 6

The "current ABBCE specifications" refers to the detector operability requirement of two detectors per level per quadrant, which Palisades has retained from its inception with the original INCA methodology supplied by Combustion Engineering. This requirement assures accurate monitoring of quadrant power tilt. Each Combustion Engineering NSSS plant has some variation of this requirement to effectively monitor QPT. Some plants use the CECOR methodology with Technical Specifications that require them to maintain one detector per level per quadrant and a minimum of six quadrant power tilt estimates with a minimum of one estimate at each of three levels. This could be accomplished by one operable detector string with three operable detectors in a given quadrant, assuming it is part of a four-way symmetric set. Another plant uses the CECOR methodology with Technical Specifications that require them to maintain two four-way symmetric sets. Three of four detectors must be operable for the string to be operable. Another plant also uses CECOR but their requirements are slightly different with a minimum of two detector strings per quadrant. Again, three of four detectors must be operable for the string to be operable.

NRC Question No. 7

Regarding the fourth paragraph of Section 4.3.3 (page 26) of the report, please describe the "base test case" in detail. Also, address the following:

a) *Please explain why the five sets of failed detectors cover all possible combinations of failed sets.*

b) *Please describe the five sets of 18 failed detectors and the statistical analysis associated with the five sets of failed detectors.*

c) *Please explain why the effects of the radial power tilts for the 50-percent failed detectors were not examined. Is not this the objective of the analysis?*

d) *Please provide a comparison of the statistical results as tabulated in reference [PID961] of the 25-percent loss of detectors versus the 50-percent loss of detectors and explain how the elimination of assemblies with RPFs<1 support these results.*

Response to Question No. 7

In section 4.4.3 the "Base Case" for each cycle represents a hot full power (HFP) Middle-of-Cycle (MOC) case with close to a full complement of operable detectors (180) for the remaining 36 strings we plan to load from cycle 15 forward. Typically, a few detectors fail each cycle for various reasons. The seven detectors actually eliminated from cycle 15 were also removed analytically from the uncertainty analysis, and assemblies with relative power fractions (RPF) less than 1.0 were included, since we are interested in the effects of large numbers of detector failures on these 36 strings. The Base Cases for cycles 12 to 14 are represented in the latest PIDAL-3 submittal in Figure 4.5c, "12F0", "13F0", and "14F0".

a) The five sets of failed detectors do not explicitly cover all possible combinations of failed sets of detectors. In the original PIDAL submittal, approved in April of 1992, we determined that trying to analyze every possible combination was prohibitive and unnecessary in determining the effects of large numbers of detector failures. Five sets of detectors with 25% failed were randomly selected for determining the penalty to be applied. Subsequently, in the first PIDAL-3 submittal in 1996 we also employed the same methodology in failing five sets of detectors with 25% failed. As in the original PIDAL submittal it was determined that the number of detectors failed is not as important as which detectors are failed. Misbehaving detectors, which may

be failing or misaligned, will produce larger uncertainties than well-behaved detectors. As you approach 50% operability by removing well-behaved detectors from the pool of operable detectors, the overall uncertainty increases. Naturally, the opposite is true if misbehaved detectors are removed. This is why some of the cases in Figure 4.5c have uncertainties higher than the base case and some have uncertainties lower.

b) The five sets of 18 failed detectors were randomly generated using Microsoft EXCEL. The EXCEL parameters were set to produce 36 numbers between 1 and 43 (The highest detector number of the 36 applicable strings). Since EXCEL will repeat numbers, 36 total numbers were required to produce 18 random failures. Analysis [PID992], sent to the NRC in our August 11, 2000, submittal, shows a list of the numbers in Appendix 7.8, page 4. Moving down the list, the highlighted numbers represent the randomly selected 18 failed detectors.

The statistical analysis associated with the five sets of failed detectors is listed in Figure 4.5c as "12F1" to "12F5", "13F1" to "13F5", and "14F1" to "14F5". From the list of numbers in the last three columns of Figure 4.5c, the largest deviation between the base and test cases were as follows:

F_{Q_T} Cycle 13 "13F2" - "13F0" or 0.0377 - 0.0349 = 0.0028
F_R^T Cycle 14 "14F1" - "14F0" or 0.0334 - 0.0280 = 0.0054
F_R^A Cycle 14 "14F1" - "14F0" or 0.0285 - 0.0212 = 0.0073

The numbers as applied in Figure 4.5a in "Note 3" were rounded up to 0.0030, 0.0055, and 0.0075 respectively. These are simply added to the final uncertainties as they are calculated.

c) The effects of the radial power tilts in general cannot be examined since we do not have actual measured detector data with tilts (i.e. dropped rod). All of the radial power tilt calculations were examined using theoretical detector data supplied by SIMULATE-3. The theoretical detector values were determined with independent full core XTG and SIMULATE-3 cases, and then the actual plant detector signals were overlaid with these theoretical values. The original PIDAL and PIDAL-3 models were then run, and the results of the radial tilt calculations are listed below in Response to Question 9. As the results indicate, PIDAL-3 can reproduce the SIMULATE-3 theoretical detector powers with no standard deviation for the F(s) and F(sa) components, since SIMULATE-3 uses a full core model. The F(r) and F(z) components are consistent with the other cases. Refer to the accompanying PIDAL-3 Uncertainty Analysis Manual for explanations of each component.

d) The following Table shows a comparison of the Uncertainty Analysis results from analysis [PID991] with 25% of the detectors failed and [PID992] with 50% of the detectors failed. Since the results for [PID961] covered only cycles 9 through 11, while [PID991] covers cycles 9 through 14 using the same CASMO-3 model, the following comparison was made between [PID991] and [PID992]. The results for [PID991] and [PID992] came from the April 21, 2000, PIDAL-3 submittal, Figures 4.5a-b.

	25% Failed [PID991]	50% Failed [PID992]
Cycle 9 Peak Assembly (F_R^A)	0.0201	0.0239
Cycle 9 Peak Pin (F_R^I)	0.0364	0.0301
Cycle 9 Peak LHGR (F_Q)	0.0429	0.0344
Cycle 10 Peak Assembly (F_R^A)	0.0267	0.0248
Cycle 10 Peak Pin (F_R^I)	0.0399	0.0305
Cycle 10 Peak LHGR (F_Q)	0.0456	0.0343
Cycle 11 Peak Assembly (F_R^A)	0.0314	0.0331
Cycle 11 Peak Pin (F_R^I)	0.0430	0.0366
Cycle 11 Peak LHGR (F_Q)	0.0482	0.0386
	25% Failed [PID991]	50% Failed [PID992]
C11 Xenon Peak Asm. (F_R^A)	0.0345	0.0360
C11 Xenon Peak Pin (F_R^I)	0.0454	0.0390
C11 Xenon Peak LHGR (F_Q)	0.0561	0.0417
Cycle 12 Peak Assembly (F_R^A)	0.0225	0.0279
Cycle 12 Peak Pin (F_R^I)	0.0377	0.0326
Cycle 12 Peak LHGR (F_Q)	0.0412	0.0336
Cycle 13 Peak Assembly (F_R^A)	0.0227	0.0267
Cycle 13 Peak Pin (F_R^I)	0.0379	0.0319
Cycle 13 Peak LHGR (F_Q)	0.0426	0.0337
Cycle 14 Peak Assembly (F_R^A)	0.0184	0.0230
Cycle 14 Peak Pin (F_R^I)	0.0356	0.0296
Cycle 14 Peak LHGR (F_Q)	0.0444	0.0374

As expected the peak assembly measurement uncertainties (F_R^A) are comparable, and the peak pin (F_R^T) and linear heat generation rate (LHGR) (F_Q) measurement uncertainties are lower given the improvements made by CASMO-4 with the pin power measurement uncertainty (F_L). Figures 4.5a-b show the pin power

measurement uncertainty (F_L) in column 5. The original PIDAL used 0.0135, PIDAL-3 with CASMO-3 uses 0.0163, and PIDAL-3 with CASMO-4 uses 0.0100. Additionally, the axial synthesis uncertainty component (F_z) is lower for CASMO-4 and thus further improves the LHGR uncertainty.

The elimination of assemblies with relative power fractions (RPF) less than 1.0 is explained in detail in the PIDAL-3 submittal, section 4.4.1. The elimination of the peripheral assemblies with RPFs less than 1.0 improves the accuracy for higher power assemblies, which in turn, tends to decrease the standard deviations and the degrees of freedom.

THE PIDAL-3 FULL CORE SYSTEM

UNCERTAINTY ANALYSIS MANUAL

Palisades Nuclear Engineering Department

Revision 00	P*PID*89002 Rev 0	06/1989
Revision 01	P*PID*89002 Rev 1	10/1989
Revision 02	EA-GAB-90-06 Rev 0	08/1990
Revision 03	EA-TCA-93-01 Rev 1	10/1993
Revision 04	EA-PID-95-02 Rev 0	05/1995
Revision 05	EA-PID-96-01 Rev 0	07/1996
Revision 06	EA-PID-96-02 Rev 0	06/1997
Revision 07	EA-PID-99-02 Rev 0	10/1999

ABSTRACT

The Uncertainty Analysis Manual for the PIDAL-3 Full Core On-line Palisades Incore Detector Algorithm provides a detailed description of the individual uncertainty components associated with the PIDAL-3 methodology.

THE PIDAL-3 FULL CORE SYSTEM

UNCERTAINTY ANALYSIS MANUAL

List of Effective Pages

Revision 00	
Revision 01	Replaced By Rev 02
Revision 02	Entire Manual
Revision 03	Section 2.1,2.2,2.6,6
Revision 04	Miscellaneous Typos
Revision 05	Entire Manual
Revision 06	References
Revision 07	Entire Manual

THE PIDAL-3 FULL CORE SYSTEM

UNCERTAINTY ANALYSIS MANUAL

Table of Contents

1.0 INTRODUCTION **1**
2.0 PROGRAM INPUT **3**
2.1 References 3
2.2 Definitions 3
3.0 UNCERTAINTY ANALYSIS STATISTICAL MODEL **5**
3.1 Description Of The Uncertainty Components 5
3.2 F(s) Uncertainty Component 10
3.3 F(sa) Uncertainty Component 11
3.4 F(r) Uncertainty Component 12
3.5 F(z) Uncertainty Component 13
3.6 F(L) Uncertainty Component 14
4.0 UNCERTAINTY ANALYSIS CALCULATIONS **15**
4.1 Methodology 15
4.2 Effects on Uncertainties 16
4.3 Database 19
4.4 Results of Statistical Combinations 20
5.0 TABLES **21**
Table 5.1 Cycle 14 Summary of Statistical Data 21
Table 5.2 Cycle 13 Summary of Statistical Data 21
Table 5.3 Cycle 12 Summary of Statistical Data 22
Table 5.4 Cycle 11 Xenon Oscillation Summary of Statistical Data 22
Table 5.5 Cycles 5-7 Summary of Statistical Data for New Detectors 23
Table 5.6 Summary of Peaking Factor Uncertainties 24
6.0 FIGURES **25**

THE PIDAL-3 FULL CORE SYSTEM

UNCERTAINTY ANALYSIS MANUAL

Palisades Nuclear Engineering Department

Revision 00	P*PID*89002 Rev 0	06/1989
Revision 01	P*PID*89002 Rev 1	10/1989
Revision 02	EA-GAB-90-06 Rev 0	08/1990
Revision 03	EA-TCA-93-01 Rev 1	10/1993
Revision 04	EA-PID-95-02 Rev 0	05/1995
Revision 05	EA-PID-96-01 Rev 0	07/1996
Revision 06	EA-PID-96-02 Rev 0	06/1997
Revision 07	EA-PID-99-02 Rev 0	10/1999

ABSTRACT

The Uncertainty Analysis Manual for the PIDAL-3 Full Core On-line Palisades Incore Detector Algorithm provides a detailed description of the individual uncertainty components associated with the PIDAL-3 methodology.

THE PIDAL-3 FULL CORE SYSTEM

UNCERTAINTY ANALYSIS MANUAL

List of Effective Pages

Revision 00	
Revision 01	Replaced By Rev 02
Revision 02	Entire Manual
Revision 03	Section 2.1,2.2,2.6,6
Revision 04	Miscellaneous Typos
Revision 05	Entire Manual
Revision 06	References
Revision 07	Entire Manual

THE PIDAL-3 FULL CORE SYSTEM

UNCERTAINTY ANALYSIS MANUAL

Table of Contents

1.0 INTRODUCTION **1**
2.0 PROGRAM INPUT **3**
2.1 References 3
2.2 Definitions 3
3.0 UNCERTAINTY ANALYSIS STATISTICAL MODEL **5**
3.1 Description Of The Uncertainty Components 5
3.2 F(s) Uncertainty Component 10
3.3 F(sa) Uncertainty Component 11
3.4 F(r) Uncertainty Component 12
3.5 F(z) Uncertainty Component 13
3.6 F(L) Uncertainty Component 14
4.0 UNCERTAINTY ANALYSIS CALCULATIONS **15**
4.1 Methodology 15
4.2 Effects on Uncertainties 16
4.3 Database 19
4.4 Results of Statistical Combinations 20
5.0 TABLES **21**
Table 5.1 Cycle 14 Summary of Statistical Data 21
Table 5.2 Cycle 13 Summary of Statistical Data 21
Table 5.3 Cycle 12 Summary of Statistical Data 22
Table 5.4 Cycle 11 Xenon Oscillation Summary of Statistical Data 22
Table 5.5 Cycles 5-7 Summary of Statistical Data for New Detectors 23
Table 5.6 Summary of Peaking Factor Uncertainties 24
6.0 FIGURES **25**

1.0 INTRODUCTION

The Uncertainty Analysis Manual provides documentation of the uncertainties associated with using PIDAL-3, Palisades Incore Detector Algorithm program, for measuring the 3D full core on-line incore power distributions per [P3MM].

The PIDAL-3 methodology has evolved over several years since it was developed to replace the original Palisades one-eighth core [INCA] program. Initially, the PIDAL-3 full core solution was based on a combination of the existing [INCA] methodology and other full core measurement schemes such as [CECOR]. Over the course of development, shortcomings in the previous methods were identified, particularly in the way the full core radial power distributions and tilts were constructed. Several new techniques were employed which resulted in an improved methodology as compared to the previous systems.

In order to determine the uncertainty associated with using PIDAL-3 for monitoring the power distribution, it was again decided to draw on previous industry experience. A copy of the INPAX-II monitoring system uncertainty analysis, [EXXON], developed by the Siemens Power Corporation (formerly Exxon Nuclear and ANF), was obtained with the permission of SPC. After preliminary work, the statistical methods used by SPC were deemed adequate, with a few variations, and the uncertainties associated with PIDAL-3 were determined as described in the remainder of this manual.

With Palisades move to low leakage core designs, changes had to be made to the original uncertainty methodology to bound these cores by the NRC approved uncertainties in Technical Specifications. Since the outside assembly powers are considerably lower than the average, their percent deviations from theoretical are greatly magnified thereby increasing the overall uncertainty. The first modifications to the methodology allowed the user to manually fail low power incore instruments (ICIs). By failing the 6 outside ICIs, the user could bound a cycle to the approved uncertainties.

The present PIDAL-3 methodology modified this approach to allow the user to manually fail low power assemblies. Since any assembly with a relative power fraction (RPF) < 1.0 unnecessarily penalizes the uncertainty, and the only assemblies of interest are those with an RPF > 1.0, we chose to employ OPPD's methodology in [CCLIB] and remove all assemblies with RPFs < 1.0. This produces an uncertainty that is conservative for the core peak, but doesn't penalize it unnecessarily.

The following documentation discusses in detail the methodology used to generate the uncertainties and various factors that effect the uncertainties.

2.0 PROGRAM INPUT

2.1 References

[ANSI] American National Standards Institute Inc., 'Assessment of the Assumption of Normality (Employing Individual Observed Values)', ANSI N15.15-1974, Approved 10/1973.
[CAS4] CASMO-4 Fuel Assembly Burnup Program.
[CECOR] ABBCE, 'CECOR Fixed Incore Detector Analysis System', 06/1983.
[CCLIB] CECORLIB 3.3 Parts 1 & 2, OPPD EA-FC-94-044, 08/1995.
[CMS991] EA-CMS-99-01 Rev 0 'CMS Model Development for Cycles 1 to 15', 05/1999.
[CMS992] EA-CMS-99-02 Rev 0 'CMS Calculation of the B&W Critical Experiments', 12/1999.
[COLR] COLR, 'Core Operating Limits Report'.
[EXXON] XN-NF-83-01(P), 'Exxon Nuclear Analysis of Power Distribution Measurement Uncertainty for St. Lucie Unit 1', 01/983.
[GAB906] EA-GAB-90-06 'PIDAL Quadrant Power Tilt Uncertainty', 08/1990.
[INCA] INCA Users Manual, Nuclear Power Department, Combustion Engineering Ver. 1.0.
[OWEN] D.B. Owen, 'Factors for One-Sided Tolerance Limits and for Variable Sampling Plans', Sandia Corporation Monograph, SCR-607, 03/1963.
[PDQ] PDQ7 Program, Users Manual.
[PID3] PIDAL-3 Full Core Monitoring System.
[P3MM] PIDAL-3 Methodology Manual.
[P3UM] PIDAL-3 Users Manual.
[PID892] EA-P-PID-89002 Rev 0 'Palisades Full Core Uncertainty Analysis', 10/1989.
[PID961] EA-PID-96-01 Rev 0 'PIDAL-3 Code', 06/1996.
[PID991] EA-PID-99-01 Rev 0 'PIDAL-3 Code Update with PPC Trending', 10/1999.
[PID992] EA-PID-99-02 Rev 0 'PIDAL-3 Model Enhancements using CASMO-4', 10/1999.
[PSES] RE Walpole and RH Myers, 'Probability and Statistics for Engineers and Scientists', 2 Ed., Macmillan Publishing Co, 1978.
[RDM] Glenn F. Knoll, 'Radiation Detection and Measurement', Wiley Publishing Co, 1979.
[SIM3] SIMULATE-3 Advanced 3D Nodal Code.
[STEA] A. Hald, 'Statistical Theory with Engineering Applications', Wiley & Sons 1952, pg. 290.
[UNS3] UNSAT-3 Program, PIDAL-3 Users Manual, Attachment 13.
[XTG] XTGPWR / UJUN90 Program, Users Manual, ANF-CC-028(P) Rev. 4 Sup. 1, 10/1990.

2.2 Definitions

ICI Incore Instrument, Incore detector, or Self Powered Neutron Detector.
LHGR Linear heat generation rate (kw/ft).
PPC Palisades Plant Computer System.
RPF Relative Power Fraction or Assembly power / Average assembly power in core.
95/95 Tolerance Limit - this limit ensures that there is a 95 percent probability that at least 95 percent of the true peaking values will be less than the [PID3] measured/inferred peaking values plus the associated tolerance limit.

3.0 UNCERTAINTY ANALYSIS STATISTICAL MODEL

3.1 Description Of The Uncertainty Components

The objective is to determine the uncertainties associated with using the [PID3] program for measuring core power distributions. Therefore, the measurement uncertainties for three different measurement quantities must be determined. These three quantities are [COLR] limiting and defined as follows:

F_Q **Total Peaking Factor**. Ratio of the peak local fuel pin power to the core average local pin power. For Palisades this value is frequently written in terms of peak linear heat generation rate (LHGR).

F_R^T **Total Radial Peaking Factor**. Ratio of the individual fuel pin power to the core average pin power integrated over the total core height, including tilt.

F_R^A **Assembly Radial Peaking Factor**. Ratio of the individual fuel assembly power to the core average assembly power integrated over the total core height, including tilt.

For each of the peaking factors defined above, three separate components of the uncertainties associated with the peaking factor calculations are defined:

1) Box Measurement Uncertainty

The uncertainty associated with measuring segment powers in the detector locations.

2) Nodal Synthesis Uncertainty

The uncertainty associated with using the radial and axial power distribution synthesis techniques employed by [PID3] to calculate a nodal power. Specifically, the uncertainties associated with the radial coupling to uninstrumented locations and the axial curve fitting used to obtain an axial power shape from five discrete detector powers.

3) Pin-to-Box Uncertainty

The uncertainty associated with using the [SIM3] Local Peaking Factors (LPFs) or Pin-to-Box (PTB) Factors to represent the pin power distribution within each assembly. This uncertainty is unique in that it must be determined from critical experiments independent of all commercial reactors, since incore detectors can only determine assembly powers (through measurement and conversion of instrument tube fluxes) not individual pin powers.

Now we can mathematically redefine each of the peaking factors in terms of these components. This was accomplished by utilizing forms for the peaking factors developed by SPC. This work is documented in [EXXON] and used by Palisades with the permission of SPC.

The peaking factors, for purposes of statistical analysis, were written in the following forms:

$$F(q) = F(s) * F(r) * F(z) * F(L) \qquad 3.1a$$

$$F(rT) = F(sa) * F(r) * F(L) \qquad 3.1b$$

$$F(rA) = F(sa) * F(r) \qquad 3.1c$$

where:

F(s)	- Relative power associated with a single detector measurement
F(sa)	- Relative power associated with the average of the detector measurements within a single assembly
F(r)	- Ratio of the assembly relative power to the relative power of the detector measurements within that assembly
F(z)	- Ratio of the peak planar power in an assembly to the assembly average power
F(L)	- Peak local pin power within an assembly relative to the assembly average power

An important point to be drawn from these definitions for the peaking factors is that the F(r) value is equal to the ratio of the assembly relative power to the F(s) or F(sa) value. Thus it should be apparent that the F(s) and F(sa) terms would drop out in a mathematical sense. The F(s) and F(sa) values were retained for the statistical analysis because their respective uncertainties could be calculated directly and used to quantify the box measurement uncertainty. It can be shown that the F(s) or F(sa) terms (denominator) disappear from the F(r) statistical uncertainty term. See section 3.4.

Given the above representations for the three peaking factors of interest, the problem was to develop a method for determining the variance or standard deviation using a combination of the separate uncertainty components.

For example, the uncertainty component for F(rA) is as follows:

The peaking factor, F(rA), is defined in equation 3.1c above. Using the general form of the error propagation formula given in [RDM] pg. 131, F(rA) can be written as:

$$S_u^2 = \left(\frac{\partial u}{\partial x}\right)^2 S_x^2 + \left(\frac{\partial u}{\partial y}\right)^2 S_y^2 + \left(\frac{\partial u}{\partial z}\right)^2 S_z^2 + \ldots \qquad 3.1d$$

and substituting for u, x, and y yields:

$$S_{F(rA)}^2 = \left(\frac{\partial F(rA)}{\partial F(sa)}\right)^2 S_{F(sa)}^2 + \left(\frac{\partial F(rA)}{\partial F(r)}\right)^2 S_{F(r)}^2 \qquad 3.1e$$

From equation 3.1c the partial differentials are computed as:

$$\frac{\partial F(rA)}{\partial F(sa)} = F(r) \qquad 3.1f$$

and:

$$\frac{\partial F(rA)}{\partial F(r)} = F(sa) \qquad 3.1g$$

Substitution of the partials back into equation 3.1e gives:

$$S_{F(rA)}^2 = F(r)^2 S_{F(sa)}^2 + F(sa)^2 S_{F(r)}^2 \qquad 3.1h$$

Dividing both sides of equation 3.1h by $F(rA)^2$, which is equivalent to $(F(sa) \times F(r))^2$ gives an equation for the relative variance in F(rA) as:

$$\left(\frac{S_{F(rA)}}{F(rA)}\right)^2 = \left(\frac{S_{F(sa)}}{F(sa)}\right)^2 + \left(\frac{S_{F(r)}}{F(r)}\right)^2 \qquad 3.1i$$

It is now necessary to find a more convenient form of equation 3.1i to use for the relative variance of F(rA). This is done by using the error propagation formula and implementing a simple variable transformation as follows:

let:

$$y = \ln(x)$$

and note that:

$$\frac{\partial y}{\partial x} = \frac{1}{x}$$

Substituting into the error propagation formula:

$$S_y^2 = \left(\frac{\partial y}{\partial x}\right)^2 S_x^2 = \left(\frac{1}{x}\right)^2 S_x^2 = \left(\frac{Sx}{x}\right)^2 \qquad 3.1j$$

Note that the form of equation 3.1j is the same as the form of the individual components of equation 3.1i. Therefore, it is possible to substitute the natural logarithms in the individual variance (or standard deviation) for the actual independent variables (i.e. substitute ln(F(s)) for F(s) in equation 3.1u).

From the results of equations 3.1i and 3.1j, the following formula for the relative sample variances of F(q), F(rT) and F(rA) can be written:

$$S^2_{F(q)} = S^2_{F(s)} + S^2_{F(r)} + S^2_{F(z)} + S^2_{F(L)} \qquad 3.1k$$

$$S^2_{F(rT)} = S^2_{F(sa)} + S^2_{F(r)} + S^2_{F(L)} \qquad 3.1l$$

$$S^2_{F(rA)} = S^2_{F(sa)} + S^2_{F(r)} \qquad 3.1m$$

It should be noted that equations 3.1k-m are valid only by assuming that the individual uncertainty components which make up the overall variance for the peaking factors are independent.

After determining the sample variance for each peaking factor, it is necessary to construct sample tolerance intervals for each estimate. The general form for the tolerance limits is given in [PSES] pg. 221, as:

$$\bar{x} \pm KS \qquad 3.1n$$

where:

x	- The estimated sample bias
K	- Tolerance factor, based on interval size and number of observations
S	- Estimated sample standard deviation

For our purposes, it is necessary to define only a one-sided tolerance limit. This is because we are trying to quantify how many peaking factor measurements may be below a given limit. In addition, if it can be shown that the overall variance (or standard deviation) for each peaking factor component is made up of deviations normally distributed about zero, then the bias term becomes zero. Realizing these two points, equation 3.1n can be used to construct the following upper tolerance limits for each peaking factor:

Upper tolerance limit for F(q) + $K_{F(q)} S_{F(q)}$ 3.1o

Upper tolerance limit for F(rT) + $K_{F(rT)} S_{F(rT)}$ 3.1p

Upper tolerance limit for F(rA) + $K_{F(rA)} S_{F(rA)}$ 3.1q

PALISADES INCORE DETECTOR ALGORITHM

For this analysis, the appropriate K factors are used to determine the respective one-sided 95/95 tolerance limits. The tolerance factors (K), as a function of degrees of freedom, were taken from [OWEN].

As mentioned previously, it is necessary to determine the appropriate number of degrees of freedom for each sample standard deviation in order to obtain tolerance factors. This is accomplished by using Satterthwaite's formula, which was also used in [EXXON]. This formula is given as follows:

For a variance defined as:

$$S_0^2 = a_1 S_1^2 + a_2 S_2^2 + a_3 S_3^2 + \ldots + a_k S_k^2 \qquad 3.1r$$

The degrees of freedom are given by:

$$df_0 = \frac{S_0^4}{a_1^2 S_1^4 / dF_1 + a_2^2 S_2^4 / dF_2 + a_3^2 S_3^4 / dF_3 + \ldots + a_k^2 S_k^4 / dF_k} \qquad 3.1s$$

In terms of observations, each [PID3] run can generate a maximum 'Degrees of Freedom' as follows:

F_S	= 180	Total Detectors
F_{Sa}	= 36	Total Detector Strings
F_r and F_Z	= 204	Total Assemblies
F_L	= 96	Total Measured Pins

The degrees of freedom have to be weighted together when combined per eq. 3.1s. See [EXXON] pg. 5-6.

3.2 F(s) Uncertainty Component

The standard deviation $S_{F(s)}$ is defined as the relative uncertainty in the individual detector segment powers inferred by the full core model. Inferred detector powers are those calculated for uninstrumented assemblies by the full core radial synthesis routine as opposed to detector powers derived directly from the detector signals in instrumented assemblies.

The standard deviation $S_{F(s)}$ can be obtained by comparing equivalent inferred detector powers to measured detector powers. First, a full core power distribution is obtained based on the full core methodology described in [P3MM]. Then, one detector string is failed and the full core radial synthesis routine is repeated treating this location as uninstrumented. The failed string is again made operable with the original detector signals. This scheme of failing and replacing detector strings is repeated until inferred powers have been calculated for all strings. The $S_{F(s)}$ analysis only considers fully operable strings.

The equation for determining the standard deviation of all of the individual segment measured/inferred deviations is as follows:

$$S_{F(s)} = \sqrt{\frac{\sum D_{s_i}^2 - N_s \bar{D}_s^2}{N_s - 1}} \qquad 3.1t$$

$$D_{s_i} = \ln(F_{s_i}^I) - \ln(F_{s_i}^M) \qquad 3.1u$$

where:

N_s	- Total number of measured/inferred segment power deviations
$\bar{D}_s$	- Arithmetic mean of the individual D_{si}
F^M_{si}	- Radial normalized measured detector segment power for detector i
F^I_{si}	- Radial normalized inferred detector segment power for detector i

It should be noted that there is an underlying assumption made in using equation 3.1t to determine the individual detector segment power standard deviation. It is assumed that the uncertainty associated with inferred powers is greater than the uncertainty associated with measured powers. This assumption is supported by the fact that the inferred powers, by design, are influenced by the theoretical solution via the coupling coefficient calculation. Therefore, the inferred detector powers will contain errors induced by the theoretical nodal model as described in [P3MM] section 3.4.

Initially, this method may appear to ignore any uncertainty components associated with measurement and signal-to-power conversion errors. However, the deviations contain the measurement uncertainty because the relative difference between measured and inferred powers represents an estimate of the combined measured and calculational error.

3.3 F(sa) Uncertainty Component

The standard deviation $S_{F(sa)}$ is defined as the relative uncertainty in the average of the five inferred detector segment powers within an assembly. The measured and inferred detector segment power data used for this component comes from the same individual segment power data used for the $S_{F(s)}$ analysis. The $S_{F(sa)}$ analysis also only considers fully operable strings.

The equation used for determining the standard deviation of the string-average detector segment measured/inferred deviations is:

$$S_{F(sa)} = \sqrt{\frac{\sum D_{sa_i}^2 - N_{sa}\bar{D}_{sa}^2}{N_{sa} - 1}} \qquad 3.1v$$

$$D_{sa_i} = \ln(F_{sa_i}^{I}) - \ln(F_{sa_i}^{M}) \qquad 3.1w$$

where:

N_{sa}	- Total number of measured/inferred segment power deviations
$\bar{D}_{sa}$	- Arithmetic mean of the individual D_{sai}
F^{M}_{sai}	- Radial normalized measured detector segment power for detector i
F^{I}_{sai}	- Radial normalized inferred detector segment power for detector i

3.4 F(r) Uncertainty Component

The standard deviation $S_{F(r)}$ is defined as the relative uncertainty associated with the radial synthesis from measured powers to inferred powers. This component assumes that the radial coupling methods employed are valid and accurate for inferring detector powers in uninstrumented assemblies, and that the resultant integrated assembly powers are similar to known values.

The data for this component is obtained by overlaying measured detector powers with theoretical detector powers already calculated in the full core model. The full core power distribution is calculated based on the theoretical detector powers. The resultant integrated assembly powers are then compared with the original theoretical radial power distribution. The difference will represent the error in the radial synthesis method.

The equation used for calculating the $S_{F(r)}$ standard deviation is:

$$S_{F(r)} = \sqrt{\frac{\sum D_{r_i}^2 - N_r \bar{D}_r^2}{N_r - 1}} \qquad 3.1x$$

$$D_{r_i} = \ln(F_{r_i}^I) - \ln(F_{r_i}^M) \qquad 3.1y$$

where:

N_r	- Total number of measured/inferred assembly power deviations
$\bar{D}_r$	- Arithmetic mean of the individual D_{ri}
F^M_{ri}	- Radial normalized measured assembly power for assembly i
F^I_{ri}	- Radial normalized inferred assembly power for assembly i

As mentioned in section 3.1, the F(r) uncertainty term is mathematically the ratio of assembly relative power to the power of the detector measurements in an assembly. From equation 3.1y, it can be shown that the detector measurement term (either F(s) or F(sa)) drops out of the formula. This is because the difference in the natural logarithms is identically equal to the natural logarithm of the inferred F(r) term divided by the measured F(r) term. Thus the denominators of each term will cancel out.

3.5 F(z) Uncertainty Component

The standard deviation $S_{F(z)}$ is defined as the relative uncertainty associated with the axial synthesis from five detector segment powers to twenty-five axial nodal powers. This is the uncertainty associated with the axial curve fitting technique, including calculation of axial boundary conditions.

The data for this component is again obtained by overlaying measured detector powers with theoretical detector powers already calculated in the full core model. The full core power distribution is calculated based on the theoretical detector powers. The resultant assembly peak nodal power is then compared with the original theoretical peak nodal power. The difference will represent the error in the axial synthesis method.

The equation used for calculating the $S_{F(z)}$ standard deviation is:

$$S_{F(z)} = \sqrt{\frac{\sum D_{z_i}^2 - N_z \bar{D}_z^2}{N_z - 1}} \qquad 3.1z$$

$$D_{z_i} = \ln(F_{z_i}^I) - \ln(F_{z_i}^M)$$

where:

N_z	- Total number of measured/inferred assembly power deviations
$\bar{D}_z$	- Arithmetic mean of the individual D_{zi}
F^M_{zi}	- Axial normalized measured assembly power for assembly i
F^I_{zi}	- Axial normalized inferred assembly power for assembly i

3.6 F(L) Uncertainty Component

The standard deviation $S_{F(L)}$ is defined as the uncertainty associated with the PTB factors supplied by [SIM3]. This factor is the ratio of assembly peak pin power to average pin power for that assembly. To determine the uncertainty associated with the PTB factors, we benchmarked our in-house [SIM3] model to the industry standard B&W Critical Experiments in [CMS992].

B&W performed a series of critical experiments with various configurations of fuel pins, poison pins, and control rod water holes. Six of these cores have been used by the industry to benchmark in-house methodologies using [SIM3]:

The equation used for calculating the $S_{F(L)}$ standard deviation is:

$$S_{F(L)} = \sqrt{\frac{\sum D_{L_i}^2 - N_L \bar{D}_L^2}{N_L - 1}} \qquad 3.1zz$$

$$D_{L_i} = \ln(F_{L_i}^I) - \ln(F_{L_i}^M)$$

where:

N_L	- Total number of measured/inferred pin power deviations
$\bar{D}_L$	- Arithmetic mean of the individual D_L
F^M_{Li}	- Radial normalized measured pin power for pin i
F^I_{Li}	- Radial normalized inferred pin power for pin i

Cores 1, 12, and 18 contain 32 measured pin powers each with no gadolinia pins.
Cores 5, 14, and 20 contain 32 measured pin powers each with gadolinia bearing pins.
Cores 1, 5, 12, and 14 contain 1×1 control rod water holes evenly distributed.
Cores 18 and 20 contain 2×2 control rod water holes evenly distributed.
None of the cores have control rods inserted.

We modeled all of the cores using [CAS4] and [SIM3] 2×2 nodal models. There is a significant penalty incurred by using a 1×1 model instead of a 2×2 model given the high leakage of these very small cores. Since all of our cycle specific models are 1×1, a comparison between a 1×1 and 2×2 cycle specific model was performed in [CMS992].

Because Palisades has cruciform control rods and wide water gaps, there is concern over whether these cores are representative. Considering the size of the 2×2 water holes and the good agreement [SIM3] has around these locations, we determined that these cores are adequate for the Palisades core.

Finally, we chose to use the gadolinia pin cores exclusively in determining the uncertainty since the NRC prohibited SPC from attempting to average all 6 cores ($S_{F(L)} = 0.01$).

4.0 UNCERTAINTY ANALYSIS CALCULATIONS

4.1 Methodology

In order to determine the uncertainties associated with the [PID3] full core monitoring model, it was necessary to employ the appropriate statistical model. The NRC required Palisades to use a previously approved methodology, so we chose Siemens methodology as described in section 3.

Two computer codes and EXCEL are used to generate the statistical analysis data:

The PIDAL-3 program is used to determine the measured and inferred full core ICI powers and power distributions required. The [PID3] program fails each ICI string one at a time, and recalculates the power distribution based on inferred data. The uncertainty analysis data is written to the uncertainty file described in [P3UM] attachment 9.

The UNSAT-3 program is used to calculate the F(s), F(sa), F(r), and F(z) uncertainty components. The EXCEL spreadsheet, **eacms9902.xls**, was used in [CMS992] to calculate the F(L) uncertainty component. [UNS3] reads the Uncertainty file generated by the [PID3] program statistical analysis routines and calculates the deviations, means and standard deviations required by this analysis. [UNS3] also sets up histogram data files for figure plotting. [P3UM] attachment 13 describes the input requirements to [UNS3].

The EXCEL spreadsheet, **uncert.xls**, was used in [PID992] to determine the overall uncertainties along with the various effects listed below. The results of the computer cases with the individual component uncertainties are combined in order to determine the overall uncertainties as defined by the statistical model in section 3.

Included in this analysis was a study of various effects on the final uncertainties such as:

1) Low Leakage Cores
2) Poolability and Normality of Data
3) Failing Large Numbers of Incore Instruments
4) Radial Power Tilts
5) Large Axial Offsets

The results are discussed in section 4.2.

4.2 Effects on Uncertainties

Low Leakage Cores

Since the inception of low leakage core designs, one of the consequences is that the uncertainties for low power assemblies with relative power fractions (RPF) < 1.0 are inflated due to higher percent deviations given the same absolute deviation. One possible solution is to use absolute differences instead of percent differences, but the absolute differences in low power assemblies is small compared to average assemblies and would not be conservative. The uncertainty analysis methodology was not changed in order to comply with the NRC expectation that a previously approved methodology be used. The alternative is to eliminate all assemblies with a RPF < 1.0. Since the assemblies of interest have RPFs > 1.0, this produces a representative uncertainty that is conservative for peak assemblies, but not so conservative as to penalize the peak unnecessarily.

Poolability and Normality of Data

Before combining data in a statistical analysis, the data must be tested for poolability. Two questions must be answered: First, should the data be poolable? Second, does it make sense? The widely accepted Bartlett Test can be used to determine poolability of data within each cycle and across the cycles as described in [STEA].

In order for data to be poolable, it must be independent and devoid of trends. First, the data generated by the PPC is predictable at steady-state conditions regardless of how often the data is sampled. Therefore, we have truly dependent data and one could significantly increase the degrees of freedom by sampling more data points. This is true of all nuclear plants and is also the case with the original PIDAL uncertainties generated by pooling cycles 5, 6, and 7. Second, since the inception of low leakage core designs, BOC uncertainties tend to be higher than EOC uncertainties since the cores are more heterogeneous at BOC and become more homogeneous at EOC after the peaks have burned out.

With this in mind, it appears that Palisades is unable to pool data within a cycle let alone between cycles. If we use fewer time points across the cycle, we produce more independent data and reduce the degrees of freedom. By sampling approximately every 1000 MWD/MTU (once a month), we believe the data is independent, and we have significantly reduced the degrees of freedom. The much lower degrees of freedom is also very conservative. The [SIM3] model produced a much flatter assembly radial power RMS deviations across the cycles compared to [XTG]. Poolability across cycles 5, 6, and 7 was deemed possible given the similarity in core designs and cycle length.

For the normality test, as described in [ANSI], we used the W test for small sampling sizes (< 50) or the D-prime test for large sampling sizes. If the data passes the normality test the zero basis assumption in section 3.1 holds.

Failing Large Numbers of Incore Instruments

Current Palisades Technical Specifications require that 75% of all possible ICI locations, with a minimum of two ICIs per core level per quadrant be working in order to declare the incore monitoring system operable. The latest submittal per [PID991] and [PID992] requires 50% operability of the 36 remaining ICI locations.

[EXXON] came to the conclusion that the accuracy of an incore monitoring system or methodology depended more on which detectors were operable than on the total number operable. [EXXON] also concluded that it was best to use all available data points in determining the individual component uncertainties, and therefore, did not go into great detail investigating the effects of large numbers of incore failures on the measured/inferred power distribution. These conclusions are valid because, for random detector failures, there is an equal probability that the well behaved detectors and the non-well behaved detectors would fail.

In order to prove these conclusions, it would be necessary to test every possible combination of failed detectors for a large set of power distributions. From a computational standpoint, this is not practical. Therefore, a test was devised to verify that incore failures resulting in 50% detector operability would produce accurate measurements.

A base test case was chosen at the middle of cycles 12, 13, and 14, and the results for each of the component uncertainties were recorded. Five sets of 18 failed incore strings were then chosen using a random number generator in EXCEL. The statistical analysis was repeated for each of the 5 failed sets. The results of the 5 sets were compared to the base case. The maximum positive deviations were identified and bounding values were added to each of the uncertainties across all of the cycles. The effects of large radial power tilts with 50% of the detectors failed were not examined. The inception of the [SIM3] full core coupling calculations in [PID961], and the elimination of assemblies with RPFs < 1.0 significantly reduced the consequences of loosing 25-50% of the detectors from the original submittal with tilt.

The uncertainty analysis for cycles 9 to 14 already eliminates the operable detectors with RPFs less than 1.0, and no effect on uncertainties was observed for the [PID961] cases run examining tilted cores and 25% detector failures. In [PID992], penalties with 50% of detectors failed is comparable to [PID892] with 25% of detectors failed.

Based on these results, the uncertainties associated with the [PID3] system documented by this report are valid for an incore monitoring system operable with up to 50% of its 180 remaining incore detectors failed.

Radial Power Tilts

The original PIDAL methodology in [PID892] determined the F(s) uncertainty component for power distributions with quadrant power tilts up to 5%. The Palisades Technical Specifications allow for full power operation with quadrant power tilts of up to 5%.

The F(s) uncertainty component was recalculated for radial tilted cores in [GAB906]. The results showed that in all cases the F(s) value (0.0277) was bounding for quadrant power tilts up to 2.8%. It was also found that the F(s) value depended strongly on the direction and magnitude of the oscillation causing the power tilt. For cores oscillating about the diagonal core axis, the F(s) value was valid for tilts up to 5%. For oscillations about the major core axis, the F(s) value was valid for tilts up to 2.8%. Since the Palisades Technical Specifications allow for full power operation with quadrant power tilts of up to 5%, and it was clear that the overall PIDAL uncertainties were only valid for tilts up to 2.8%, it was necessary to derive a second set of uncertainties for tilts above 2.8%.

With the inception of [SIM3] in [PID961], radial power tilts between 2.8% and 5.0% do not require additional uncertainties since [SIM3] and [PID3] can monitor the full core including dropped control rods. The major limitation of the original submittal was a quarter core [XTG] model, and quarter core [PDQ] W-primes and LPFs. No effect on uncertainties was observed in the [PID961] and [PID992] cases, which examined tilted cores up to 5%.

Large Axial Offsets

The [PID961] and [PID992] uncertainty analyses both contain an actual power transient, which produced a xenon driven power oscillation. The movement of control rods and changes in boron concentration have the greatest effect on [SIM3]'s ability to reproduce the transient. The major limitation is due to the frequency of snapshots from the PPC (1 per hour). Too many evolutions can occur within each hour for [SIM3] to accommodate over the entire transient. For example, control rod movements 10 minutes passed the hour produce very different results than those 10 minutes to the hour. Therefore, as a transient continues [PID3] and [SIM3] begin to diverge. Fifteen minute time steps are currently available with the PPC and will improve the uncertainties.

4.3 Database

The original PIDAL database used for the NRC approved uncertainty analysis was generated using measured and predicted power distributions from [PID892] for cycles 5, 6, and 7. For the F(s), F(sa) and F(r) uncertainty components a total of 54 cases were run, equally distributed over the three cycles. Two separate cycle 7 statistical runs were then performed. The first considered the entire compliment of detector data, including fresh and reused incores, and the SPC revised cycle 7 [INCA] W-prime library. The second cycle 7 set was then generated omitting the reused detectors. The F(L) uncertainty component was supplied by Siemens using [PDQ].

The original PIDAL database also included a total of 22 cases from [PID892] in order to generate data for the F(z) uncertainty component. Of these 22 cases, 11 were selected from cycle 7. These 11 cases were selected at approximately equal intervals over the entire cycle. The other 11 cases were run for a hypothetical EOC 7 xenon oscillation. These cases were generated in order to include off-normal axial power shapes in the uncertainty analysis. The hypothetical EOC 7 xenon oscillation produced axial offsets of ± 40%. It is reasonable to assume that axial peaking uncertainties as a result of slight flux depressions caused by fuel assembly spacer grids would be small, compared to the off-normal axial shapes being investigated, and therefore these fluctuations are ignored by this analysis.

The original PIDAL database also included a total of 18 cases from [GAB906] in order to determine the measurement uncertainties for radial tilted cores. All of these cases used [XTG] theoretical detector powers from two full core dropped rod induced transient scenarios. The first 6 cases involved a tilt induced by dropping a group 4 control rod, while the second 6 cases involved a tilt induced by a group 3-outer control rod. The final 6 cases involved dropping these same 2 control rod groups in each of the remaining 3 quadrants. The first 6 cases corresponded to peak quadrant power tilts of 10%, 7.6%, 5.6%, 2.9%, 1.6% and 0.3% respectively. These cases were selected because they covered the spectrum of tilted cores up to 10%. Concentration on tilts up to 5% is greater because it is over this range that the reactor may be operated without reducing power or correcting the tilt. The second 6 cases all lie within the 5% tilt range.

The latest PIDAL database used for the NRC approved uncertainty analysis was generated using measured and predicted power distributions from [PID992] for cycles 9 to 14, with emphasis on cycles 12, 13, and 14. For the F(s), F(sa), F(r), and F(z) uncertainty components a total of 41 cases were run for cycles 9, 10, and 11, and 50 cases were run for cycles 12, 13, and 14, equally distributed over the six cycles, with RPFs < 1.0 and misaligned ICIs eliminated. This database also included 6 reruns of these 50 cases for cycles 12, 13, and 14. The first rerun produced the 3 base cases which include only the 36 ICI strings Palisades intends to load for cycle 15 and beyond, including the misaligned ICIs. The next 5 reruns over the 3 cycles involved failing 50% of the operable ICIs, or 18 ICI strings, in 5 separate scenarios with randomly chosen ICI strings. The misaligned ICIs were included since all of the ICIs are equally weighted for failure probability. Finally, 22 cases were run for an actual EOC 11 xenon oscillation, and 13 cases were run for each MOC 11 dropped control rod covering a quadrant. Both were originally developed in [PID961].

4.4 Results of Statistical Combinations

Tables 5.1 to 5.3 contain a summary of the statistical calculations for cycles 14, 13 ,and 12. Table 5.4 contains a summary of the statistical calculations for the cycle 11 xenon oscillation. Table 5.5 contains a summary of the statistical calculations for cycles 5, 6, and 7. Table 5.6 contains a summary of the statistical calculations for all of the cycles and the resulting peaking factor uncertainties.

Figures 6.1 to 6.12 are deviation histograms corresponding to the cycles 14, 13, and 12 uncertainty component standard deviations. Figures 6.13 to 6.16 are deviation histograms corresponding to the cycles 5, 6, and 7 uncertainty component standard deviations. From the histograms and means presented, it is apparent that the data is normal and unbiased. One interesting point to note is that the F(r) data is not biased as SPC had found it to be. They explained their bias as being induced by using data sets that were not normalized. The PIDAL data used was radial normalized so the PIDAL result seems to support the SPC assumption. Cycle 13 and 14 show F(r) to have an abnormal distribution. It was discovered that the axial blankets introduced have caused this abnormal distribution. If the bottom and top nodes are eliminated from the statistical analysis the distribution should return to normal (Nodes 1 and 25). No bias has been incorporated at this time, since cycle 14 is considerably better than cycle 13. Cycle 15 data should be analyzed before a decision is made.

Table 5.5 also contains the results of the F(z) statistical calculations using cycle 7 data. The first 11 elements were taken from the simulated xenon oscillation data. The last 11 elements correspond to actual data equally spread out through cycle 7. Note that element 20 was from an actual dropped rod transient. Figure 6.16 shows a histogram for the F(z) deviation data. From this histogram, the data appears generally normal but the mean deviation indicates a bias of 0.9%. Since this bias is negative, the PIDAL model is over-predicting the peak and is therefore conservative. This is similar to the result obtained by SPC.

Table 5.6 contains 3 sets of tolerance limits determined as the Technical Specification limits for F(q), F(rT) and F(rA) based on cycles 5, 6, and 7. The first set of tolerance limits is based on data from all three cycles, excluding the cycle 7 reused detector data, and is valid only for reload cores with all fresh incore detectors. The second set is based entirely on cycle 7 data and is valid only for reload cores, which contain fresh and once-burned incore detectors. The third set is based on theoretical data and is valid when quadrant power tilt, as measured by PIDAL, exceeds 2.8%. In addition, cycles 9 to 14 data from [PID9902] are also listed for comparison and to determine a new limit for F(q), F(rT), and F(rA) when the Improved Technical Specifications are issued and the tolerance limits are moved to the [COLR]. Though F(rA) has been eliminated for cycles 15 and beyond, the limit continues to be calculated as an assembly power measurement uncertainty. The new [COLR] limits will be:

F(q) = 0.0425
F(rT) = 0.0400
F(rA) = 0.0375

5.0 TABLES

Table 5.1 Cycle 14 Summary of Statistical Data

Case	Avg Dev	RMS Dev	F(s)		F(sa)		F(r)		F(z)	
			St Dev	Observ	St Dev	Observ	St Dev	Observ	St Dev	Observ
1	-0.16	1.43	0.0142	110	0.0080	22	0.0035	128	0.0007	128
2	-0.19	1.43	0.0142	110	0.0081	22	0.0035	128	0.0008	128
3	-0.21	1.45	0.0144	110	0.0086	22	0.0034	128	0.0008	128
4	-0.17	1.45	0.0147	105	0.0083	21	0.0033	128	0.0009	128
5	-0.18	1.42	0.0143	105	0.0079	21	0.0032	128	0.0014	128
6	-0.13	1.43	0.0145	105	0.0079	21	0.0032	128	0.0016	128
7	-0.11	1.41	0.0143	105	0.0076	21	0.0031	128	0.0058	128
8	-0.11	1.39	0.0141	105	0.0075	21	0.0030	128	0.0081	128
9	-0.11	1.40	0.0142	105	0.0075	21	0.0029	128	0.0080	128
10	-0.11	1.42	0.0144	105	0.0078	21	0.0029	128	0.0071	128
11	-0.10	1.44	0.0145	105	0.0077	21	0.0028	128	0.0069	128
12	-0.10	1.48	0.0149	105	0.0080	21	0.0027	128	0.0067	128
13	-0.10	1.51	0.0152	105	0.0083	21	0.0028	128	0.0064	128
14	-0.13	1.60	0.0161	105	0.0087	21	0.0028	128	0.0056	128
15	-0.15	1.61	0.0161	105	0.0092	21	0.0029	128	0.0057	128
16	-0.18	1.58	0.0158	105	0.0089	21	0.0029	128	0.0057	128
17	-0.16	1.56	0.0157	105	0.0096	21	0.0031	128	0.0053	128
18	-0.19	1.46	0.0147	105	0.0093	21	0.0032	128	0.0036	128
19	-0.14	1.40	0.0141	105	0.0093	21	0.0032	128	0.0035	128
F(s)	Standard Deviation All Cases			0.0147	Mean	0.0014	Degrees of Freedom			2010
F(sa)	Standard Deviation All Cases			0.0082	Mean	0.0015	Degrees of Freedom			402
F(r)	Standard Deviation All Cases			0.0031	Mean	-0.0029	Degrees of Freedom			2432
F(z)	Standard Deviation All Cases			0.0083	Mean	-0.0048	Degrees of Freedom			2432

Table 5.2 Cycle 13 Summary of Statistical Data

Case	Avg Dev	RMS Dev	F(s)		F(sa)		F(r)		F(z)	
			St Dev	Observ	St Dev	Observ	St Dev	Observ	St Dev	Observ
1	-0.17	1.44	0.0138	105	0.0118	21	0.0051	132	0.0010	132
2	-0.20	1.40	0.0135	105	0.0119	21	0.0051	132	0.0008	132
3	-0.16	1.43	0.0135	110	0.0117	22	0.0050	128	0.0008	128
4	-0.14	1.46	0.0142	110	0.0118	22	0.0048	128	0.0008	128
5	-0.07	1.34	0.0134	115	0.0120	23	0.0046	128	0.0007	128
6	-0.06	1.26	0.0128	110	0.0110	22	0.0045	128	0.0007	128
7	-0.06	1.14	0.0116	110	0.0099	22	0.0043	128	0.0019	128
8	-0.04	1.12	0.0114	110	0.0098	22	0.0042	128	0.0036	128
9	-0.04	1.07	0.0109	110	0.0093	22	0.0040	128	0.0055	128
10	-0.03	1.03	0.0105	110	0.0087	22	0.0040	128	0.0057	128
11	-0.02	1.10	0.0112	110	0.0094	22	0.0040	128	0.0042	128
12	-0.05	1.04	0.0106	110	0.0089	22	0.0041	128	0.0029	128
13	-0.06	0.99	0.0101	110	0.0085	22	0.0043	128	0.0032	128
14	-0.07	1.01	0.0104	110	0.0089	22	0.0044	128	0.0043	128
15	-0.07	1.05	0.0107	110	0.0091	22	0.0045	128	0.0045	128
16	-0.06	1.01	0.0103	110	0.0087	22	0.0047	128	0.0047	128
17	-0.06	1.01	0.0104	110	0.0089	22	0.0048	128	0.0053	128
F(s)	Standard Deviation All Cases			0.0117	Mean	0.0007	Degrees of Freedom			1865
F(sa)	Standard Deviation All Cases			0.0099	Mean	0.0006	Degrees of Freedom			373
F(r)	Standard Deviation All Cases			0.0045	Mean	-0.0005	Degrees of Freedom			2184
F(z)	Standard Deviation All Cases			0.0076	Mean	0.0000	Degrees of Freedom			2184

Table 5.3 Cycle 12 Summary of Statistical Data

Case	Avg Dev	RMS Dev	F(s)		F(sa)		F(r)		F(z)	
			St Dev	Observ	St Dev	Observ	St Dev	Observ	St Dev	Observ
1	-0.04	1.74	0.0170	105	0.0148	21	0.0012	132	0.0010	132
2	0.02	1.61	0.0155	105	0.0134	21	0.0012	132	0.0013	132
3	-0.04	1.54	0.0148	110	0.0127	22	0.0012	136	0.0012	136
4	-0.04	1.49	0.0142	110	0.0123	22	0.0012	136	0.0022	136
5	-0.02	1.43	0.0135	110	0.0115	22	0.0012	136	0.0029	136
6	-0.04	1.42	0.0130	105	0.0110	21	0.0011	136	0.0025	136
7	-0.04	1.38	0.0126	105	0.0105	21	0.0011	136	0.0020	136
8	-0.03	1.34	0.0121	105	0.0101	21	0.0011	136	0.0013	136
9	-0.03	1.33	0.0120	105	0.0102	21	0.0009	136	0.0017	136
10	-0.02	1.35	0.0123	105	0.0105	21	0.0006	136	0.0034	136
11	-0.03	1.36	0.0124	105	0.0109	21	0.0004	136	0.0051	136
12	-0.04	1.37	0.0126	100	0.0112	20	0.0003	136	0.0037	136
13	-0.06	1.35	0.0124	100	0.0111	20	0.0003	136	0.0022	136
14	-0.08	1.33	0.0123	100	0.0109	20	0.0003	136	0.0017	136
F(s)	Standard Deviation All Cases			0.0134	Mean	-0.0011	Degrees of Freedom			1470
F(sa)	Standard Deviation All Cases			0.0113	Mean	-0.0011	Degrees of Freedom			294
F(r)	Standard Deviation All Cases			0.0009	Mean	0.0001	Degrees of Freedom			1896
F(z)	Standard Deviation All Cases			0.0054	Mean	-0.0038	Degrees of Freedom			1896

Table 5.4 Cycle 11 Xenon Oscillation Summary of Statistical Data

Case	Avg Dev	RMS Dev	F(s)		F(sa)		F(r)		F(z)	
			St Dev	Observ	St Dev	Observ	St Dev	Observ	St Dev	Observ
1	0.24	1.69	0.0182	90	0.0158	18	0.0010	140	0.0027	140
2	0.24	1.74	0.0187	90	0.0164	18	0.0013	140	0.0046	140
3	0.20	1.81	0.0195	90	0.0166	18	0.0006	140	0.0072	140
4	0.21	1.80	0.0196	90	0.0167	18	0.0006	140	0.0063	140
5	0.20	1.85	0.0201	90	0.0167	18	0.0015	140	0.0078	140
6	0.20	1.88	0.0198	90	0.0164	18	0.0012	140	0.0074	140
7	0.17	1.86	0.0197	90	0.0164	18	0.0018	132	0.0051	132
8	0.17	1.87	0.0199	90	0.0164	18	0.0008	132	0.0038	132
9	0.17	1.87	0.0199	90	0.0165	18	0.0007	132	0.0042	132
10	0.18	1.86	0.0198	90	0.0164	18	0.0007	132	0.0065	132
11	0.18	1.84	0.0195	90	0.0164	18	0.0007	132	0.0068	132
12	0.15	1.83	0.0194	90	0.0165	18	0.0006	132	0.0057	132
13	0.19	1.89	0.0193	90	0.0165	18	0.0007	136	0.0051	136
14	0.20	1.83	0.0190	90	0.0165	18	0.0021	140	0.0038	140
15	0.21	1.77	0.0188	90	0.0164	18	0.0011	140	0.0046	140
16	0.20	1.79	0.0189	90	0.0167	18	0.0011	140	0.0046	140
17	0.22	1.73	0.0187	90	0.0163	18	0.0020	140	0.0047	140
18	0.19	1.76	0.0191	90	0.0171	18	0.0011	140	0.0074	140
19	0.16	1.71	0.0184	85	0.0162	17	0.0011	140	0.0071	140
20	0.16	1.71	0.0184	85	0.0163	17	0.0011	140	0.0066	140
21	0.16	1.69	0.0182	85	0.0160	17	0.0011	140	0.0054	140
22	0.16	1.68	0.0182	85	0.0160	17	0.0012	140	0.0058	140
F(s)	Standard Deviation All Cases			0.0191	Mean	-0.0018	Degrees of Freedom			1960
F(sa)	Standard Deviation All Cases			0.0160	Mean	-0.0018	Degrees of Freedom			392
F(r)	Standard Deviation All Cases			0.0012	Mean	0.0000	Degrees of Freedom			3028
F(z)	Standard Deviation All Cases			0.0060	Mean	-0.0026	Degrees of Freedom			3028

Table 5.5 Cycles 5-7 Summary of Statistical Data for New Detectors

Case	Avg Dev	RMS Dev	F(s)		F(sa)		F(r)		F(z)	
			St Dev	Observ	St Dev	Observ	St Dev	Observ	St Dev	Observ
1	0.44	3.30	0.0324	195	0.0216	39	0.0021	51	0.0168	51
2	0.38	2.61	0.0259	190	0.0200	38	0.0021	51	0.0169	51
3	0.33	2.56	0.0254	195	0.0199	39	0.0018	51	0.0162	51
4	0.32	2.66	0.0264	190	0.0208	38	0.0018	51	0.0150	51
5	0.22	3.60	0.0356	169	0.0256	33	0.0023	51	0.0140	51
6	0.24	2.81	0.0282	165	0.0210	33	0.0024	51	0.0135	51
7	0.19	3.09	0.0314	164	0.0253	32	0.0024	51	0.0117	51
8	0.19	2.67	0.0266	177	0.0227	35	0.0024	51	0.0150	51
9	0.21	2.94	0.0295	177	0.0258	35	0.0023	51	0.0119	51
10	0.11	2.66	0.0268	177	0.0229	35	0.0025	51	0.0131	51
11	0.11	2.74	0.0271	177	0.0227	35	0.0026	51	0.0137	51
12	0.14	2.93	0.0293	167	0.0251	33	0.0026	51	0.0023	51
13	0.24	2.76	0.0275	158	0.0228	31	0.0026	51	0.0016	51
14	0.17	3.23	0.0311	152	0.0251	30	0.0024	51	0.0020	51
15	-0.05	3.26	0.0324	148	0.0270	29	0.0023	51	0.0038	51
16	-0.01	2.80	0.0280	160	0.0239	32	0.0022	51	0.0060	51
17	-0.05	3.41	0.0341	172	0.0280	34	0.0021	51	0.0108	51
18	-0.01	2.94	0.0291	161	0.0255	32	0.0021	51	0.0144	51
19	0.04	3.29	0.0336	152	0.0182	30	0.0017	51	0.0167	51
20	0.01	3.09	0.0314	163	0.0149	32	0.0018	51	0.0178	51
21	0.00	2.90	0.0294	168	0.0130	33	0.0015	51	0.0174	51
22	-0.03	3.06	0.0314	175	0.0136	35	0.0016	51	0.0149	51
23	-0.01	2.94	0.0299	175	0.0134	35	0.0020	51		
24	-0.08	2.67	0.0267	170	0.0114	34	0.0022	51		
25	-0.15	2.38	0.0238	155	0.0114	31	0.0022	51		
26	-0.15	2.37	0.0236	160	0.0110	32	0.0023	51		
27	-0.10	2.42	0.0242	160	0.0114	32	0.0023	51		
28	-0.14	2.29	0.0228	160	0.0108	32	0.0024	51		
29	-0.17	2.28	0.0226	155	0.0107	31	0.0023	51		
30	-0.15	2.22	0.0221	155	0.0106	31	0.0026	51		
31	-0.23	2.79	0.0283	145	0.0123	29	0.0026	51		
32	-0.06	3.13	0.0318	140	0.0130	28	0.0028	51		
33	-0.15	2.97	0.0306	152	0.0132	30	0.0028	51		
34	-0.18	2.34	0.0241	152	0.0124	30	0.0025	51		
35	-0.23	2.37	0.0244	152	0.0126	30	0.0026	51		
36	0.53	2.33	0.0225	155	0.0164	31	0.0014	51		
37	0.79	3.02	0.0285	160	0.0202	32	0.0015	51		
38	0.34	3.31	0.0329	150	0.0158	30	0.0018	51		
39	0.42	2.98	0.0292	155	0.0169	31	0.0017	51		
40	0.60	2.48	0.0237	155	0.0169	31	0.0017	51		
41	0.77	3.05	0.0288	160	0.0200	32	0.0017	51		
42	0.73	2.83	0.0267	155	0.0194	31	0.0018	51		
43	0.68	2.82	0.0269	165	0.0208	33	0.0021	51		
44	0.88	2.80	0.0261	155	0.0211	31	0.0021	51		
45	0.95	2.95	0.0274	150	0.0219	30	0.0022	51		
46	0.75	2.86	0.0270	150	0.0212	30	0.0023	51		
47	0.39	2.24	0.0219	140	0.0161	28	0.0025	51		
48	0.39	2.14	0.0208	155	0.0162	31	0.0026	51		
49	0.50	2.25	0.0216	160	0.0178	32	0.0025	51		
50	0.74	2.69	0.0253	165	0.0220	33	0.0026	51		
51	0.70	2.58	0.0245	165	0.0213	33	0.0026	51		
52	0.69	2.61	0.0248	165	0.0217	33	0.0025	51		
53	0.72	2.68	0.0254	165	0.0223	33	0.0025	51		
54	0.72	2.74	0.0260	160	0.0228	32	0.0024	51		
F(s)	St. Deviation All Cases			0.0277	Mean	0.0022	Degrees of Freedom			8768
F(sa)	St. Deviation All Cases			0.0194	Mean	0.0022	Degrees of Freedom			1754
F(r)	St. Deviation All Cases			0.0022	Mean	0.0022	Degrees of Freedom			2754
F(z)	St. Deviation All Cases			0.0151	Mean	-0.0086	Degrees of Freedom			1122

PALISADES INCORE DETECTOR ALGORITHM

Table 5.6 Summary of Peaking Factor Uncertainties

	Sample Variance Input for Uncertainty Components					Calculated Peaking Factor Variances			Degrees of Freedom Input for Uncertainty Components					Calculated Peaking Factor Degrees of Freedom			Tolerance Factor Input from [OWEN]			TS Tolerance Limits with 25 or 50% Failures		
Cycle	Sf(s)	Sf(sa)	Sf(r)	Sf(z)	Sf(L)	Sf(q)	Sf(rT)	Sf(rA)	Df(s)	Df(sa)	Df(r)	Df(z)	Df(L)	Df(q)	Df(rT)	Df(rA)	Kf(q)	Kf(rT)	Kf(rA)	F(q)	F(rT)	F(rA)
TS Limits																						
New	0.0277	0.0194	0.0022	0.0151	0.0135	0.0344	0.0237	0.0195	8768	1754	2754	1122	188	4826	1226	1790	1.692	1.727	1.712	0.0623	0.0455	0.0401
Used	0.0306	0.0241	0.0021	0.0151	0.0135	0.0368	0.0277	0.0242	3415	683	969	1122	188	3823	878	694	1.692	1.733	1.746	0.0664	0.0526	0.0490
Tilt	0.0393	0.0351	0.0026	0.0151	0.0135	0.0443	0.0377	0.0352	1800	360	408	1122	188	2487	460	364	1.703	1.770	1.785	0.0795	0.0713	0.0695
9	0.0140	0.0091	0.0009	0.0055	0.0100	0.0181	0.0136	0.0091	1530	306	1800	1800	96	827	270	306	1.736	1.809	1.798	0.0344	0.0301	0.0239
10	0.0142	0.0095	0.0010	0.0048	0.0100	0.0180	0.0138	0.0096	1380	276	2056	2056	96	784	271	288	1.739	1.809	1.804	0.0343	0.0305	0.0248
11	0.0172	0.0143	0.0009	0.0053	0.0100	0.0205	0.0175	0.0143	1700	340	1988	1988	96	1154	413	340	1.727	1.778	1.790	0.0386	0.0366	0.0331
12	0.0134	0.0113	0.0009	0.0054	0.0100	0.0176	0.0151	0.0113	1470	294	1896	1896	96	758	326	294	1.741	1.793	1.802	0.0336	0.0326	0.0279
13	0.0117	0.0099	0.0045	0.0076	0.0100	0.0177	0.0148	0.0109	1865	373	2184	2184	96	847	369	544	1.736	1.784	1.760	0.0337	0.0319	0.0267
14	0.0147	0.0082	0.0031	0.0083	0.0100	0.0199	0.0133	0.0088	2010	402	2432	2432	96	1212	271	531	1.727	1.809	1.760	0.0374	0.0296	0.0230
15																						
16																						
17																						
18																						
19																						
20																						
21																						
22																						
11 Xenon	0.0191	0.0160	0.0012	0.0060	0.0100	0.0224	0.0189	0.0160	1960	392	3028	3028	96	1460	470	392	1.727	1.770	1.780	0.0417	0.0390	0.0360

Cycle	Reference	Notes
New	[PID892] EA-P-PID-89002 Rev 0	1) Spreadsheet Equations from [PID892]
Used	[PID892] EA-P-PID-89002 Rev 0	2) COLR Limits based on [PID992]
Tilt	[GB905] EA-GAB-90-06 Rev 0	Fq = 0.0425 FrT = 0.0400 FrA = 0.0375
9-14	[PID992] EA-PID-99-02 Rev 0	3) Penalty for Large Number of ICI failures:
		For [PID892] the penalty for 25% failure as applied
		Fq + 0.0041 FrT + 0.0046 FrA + 0.0067
		For [PID992] the penalty for 50% failure as applied
	[OWEN] Factors for One-sided Tolerance Limits,	Fq + 0.0030 FrT + 0.0055 FrA + 0.0075
	DB Owen, March 1963, Pages 46 to 51	4) All assembly powers < 1.0 have been eliminated

6.0 FIGURES

Figure 6.1

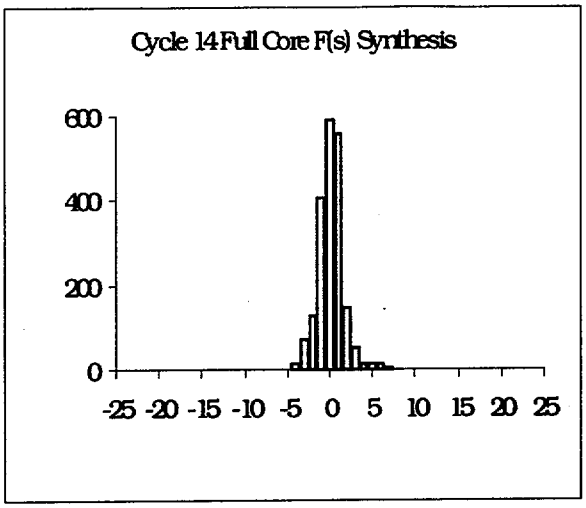

Figure 6.2

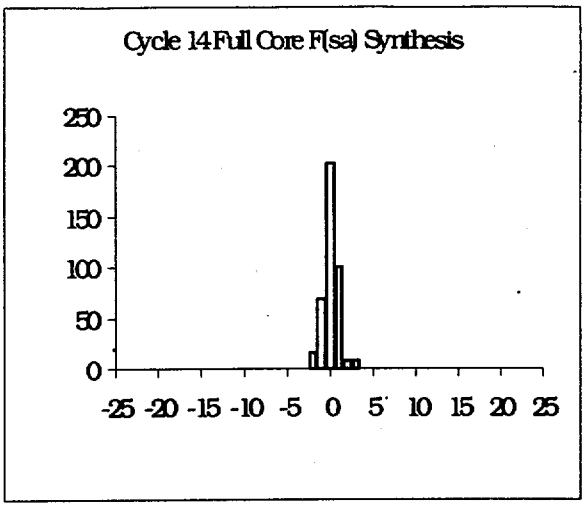

Figure 6.3

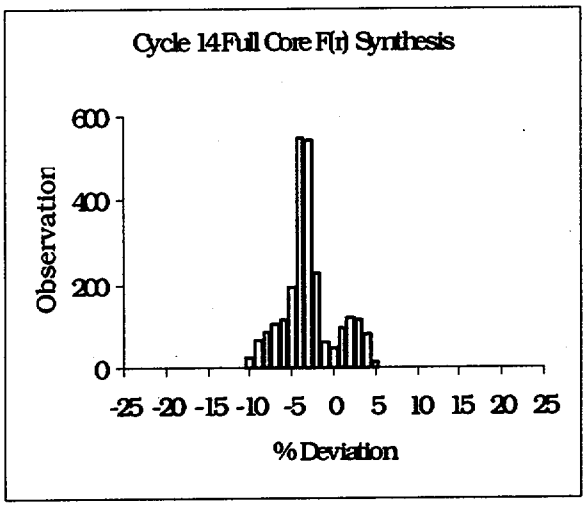

Figure 6.4

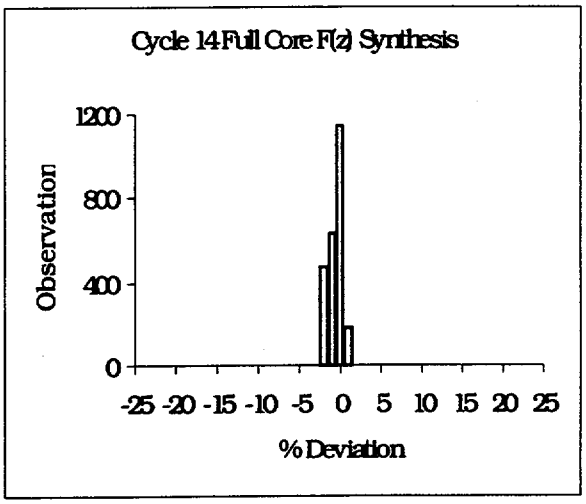

PALISADES INCORE DETECTOR ALGORITHM

Figure 6.5

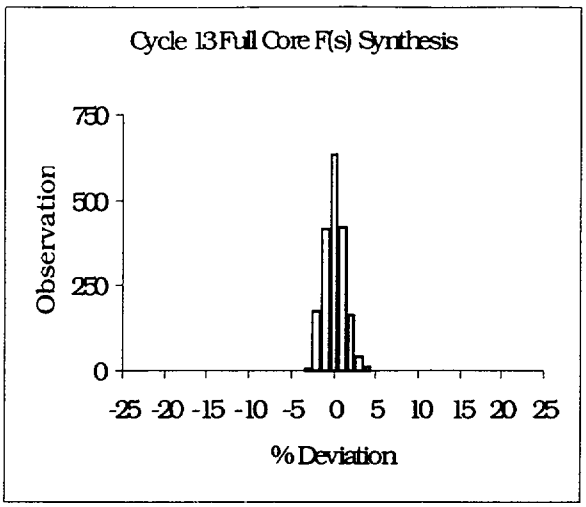

Figure 6.6

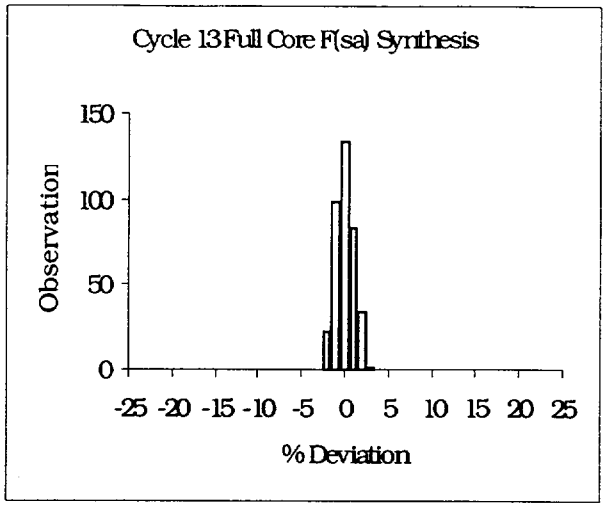

Figure 6.7

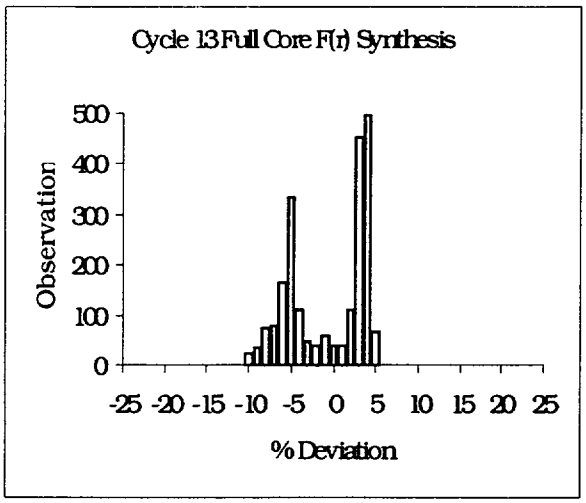

Figure 6.8

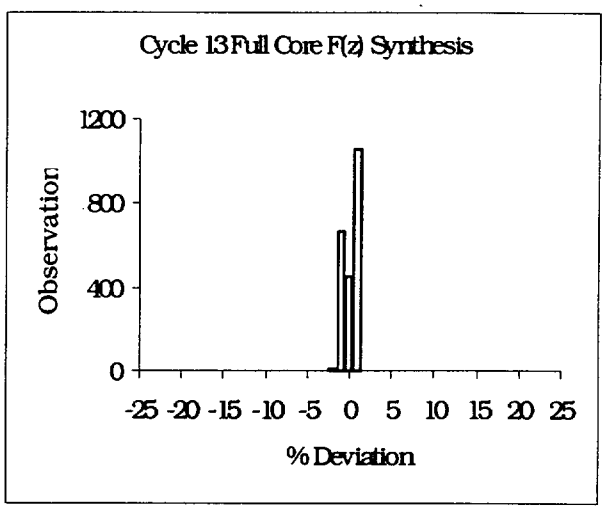

Figure 6.9

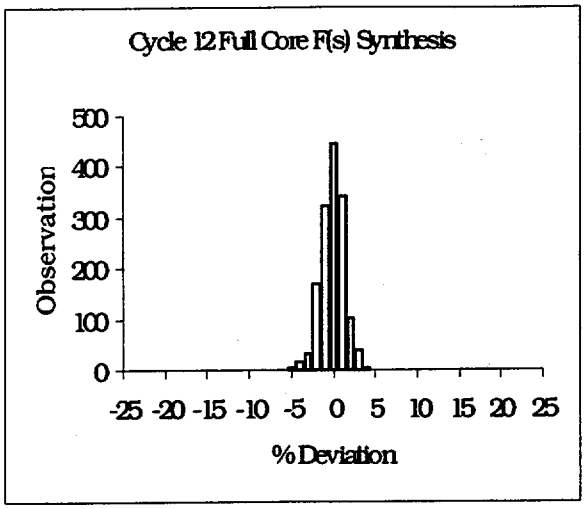

Figure 6.10

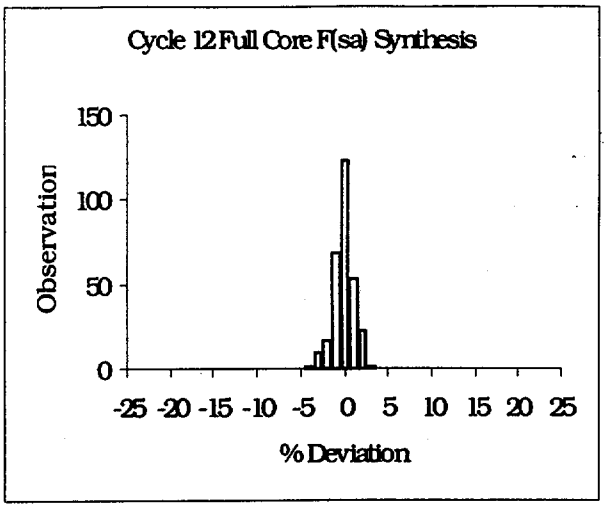

Figure 6.11

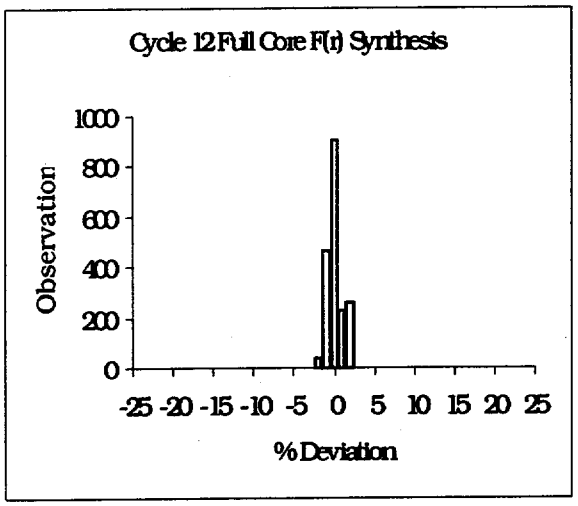

Figure 6.12

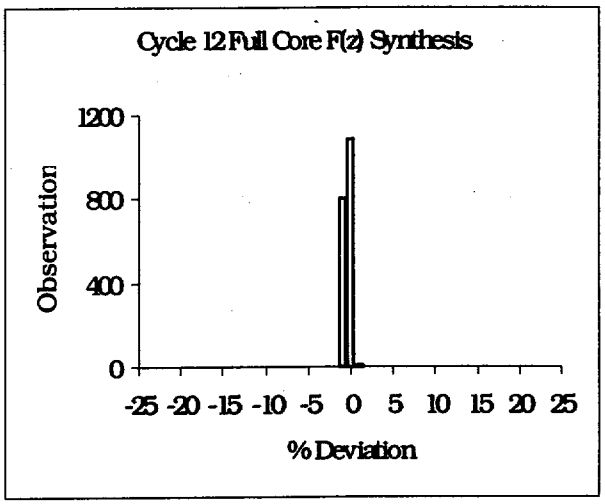

PALISADES INCORE DETECTOR ALGORITHM

Figure 6.13

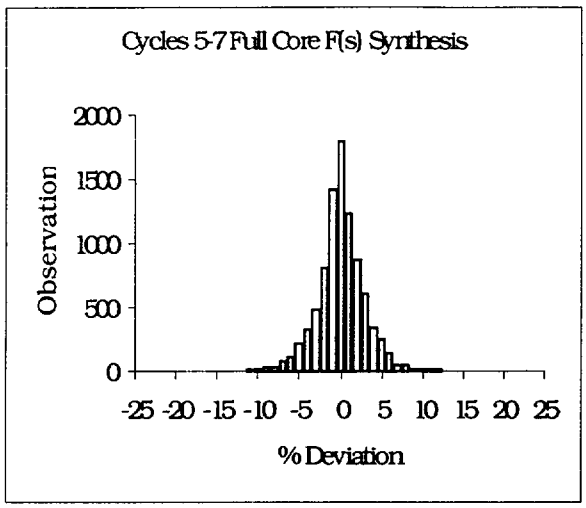

Figure 6.14

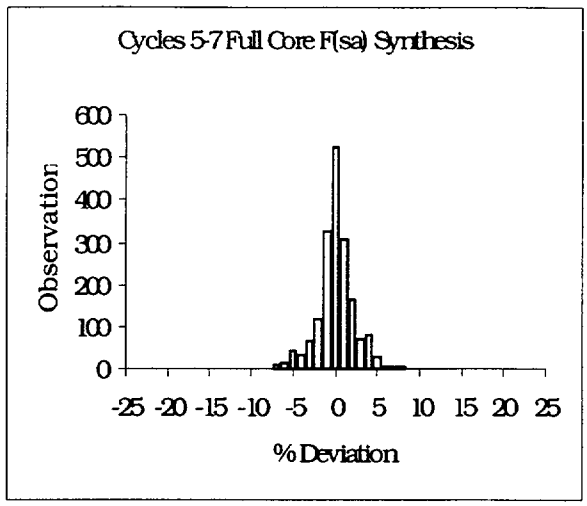

Figure 6.15

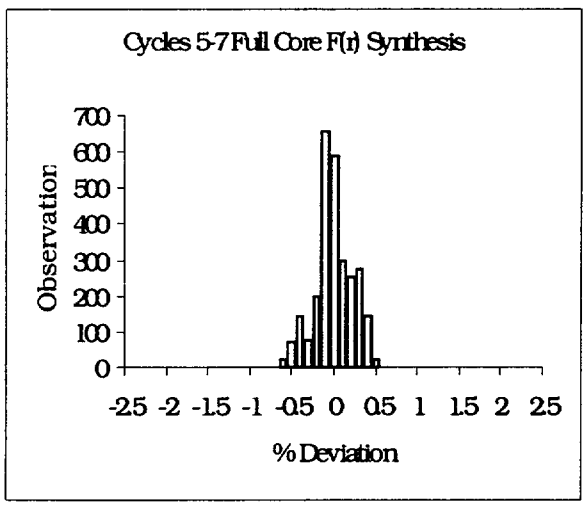

Figure 6.16

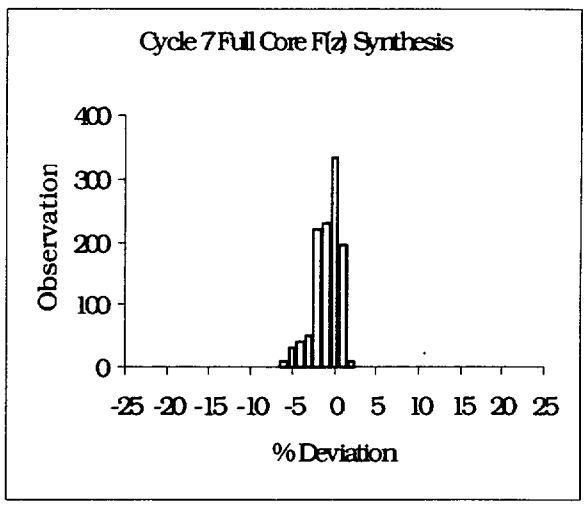

NRC Question No. 8

The last sentence of the fifth paragraph of Section 4.4.3 (page 27) of the report discusses the penalties associated with 25-percent and 50-percent detector failures. Please provide a summary of the comparisons of these two results.

Response to Question No. 8

The penalties for large numbers of detector failures were extracted from the PIDAL-3 submittal Figures 4.5a-c "Notes" and additional calculations based on [PID991] data. [PID992] represents 50% failure of 36 detector strings, [PID991] represents 25% failure of 36 detector strings, and [PID892] represents 25% failure of 43 detector strings. The following Table is a comparison of these penalties added to the uncertainty analysis results:

	Peak Asm. (F_R^A)	Peak Pin (F_R^I)	Peak LHGR (F_Q)
[PID992] Calculated	0.0073	0.0054	0.0028
[PID992] Applied	0.0075	0.0055	0.0030
[PID991] Calculated	0.0074	0.0047	0.0058
[PID892] Calculated	0.0067	0.0046	0.0041

NRC Question No. 9

The third paragraph of Section 4.4.4 (page 27) of the submittal states that, with the inception of SIMULATE-3, no additional uncertainties are required to account for power tilts of 2.8 percent and 5.0 percent. Please provide quantitative and qualitative information to support this conclusion.

Response to Question No. 9

As stated in Section 4.4.4 of the PIDAL-3 submittal, the reason for the additional uncertainty in [GAB906] is due to the quarter core XTG model used with the original PIDAL model. With the inception of a full core SIMULATE-3 model, radial power tilts with magnitudes well above 5% can be accurately modeled. The results of the radial tilt calculations are shown in analysis [PID992] Appendix 7.8 page 30. As the results indicate, PIDAL-3 can reproduce the SIMULATE-3 theoretical detector powers with no standard deviation for the F(s) and F(sa) components. The following Table is a comparison of [PID992] results from Appendix 7.8 page 30, and [GAB906] results as shown in the PIDAL-3 submittal, Figure 4.5a "Tilt" for the original PIDAL with XTG:

	F(s)	F(sa)	F(r)	F(z)	F(L)
[PID992] Appendix 7.8	0.0000	0.0000	0.0010	0.0035	0.0100
[GAB906] "Tilt"	0.0393	0.0351	0.0026	0.0151	0.0135
[PID892] "New"	0.0277	0.0194	0.0022	0.0151	0.0135

From the results above, it was determined that 2.8% QPT was the threshold at which the original PIDAL model with quarter core XTG exceeded the uncertainty values calculated with fresh or new detectors in [PID892] with no QPT. The [GAB906] values bound QPTs up to the Technical Specification limit of 5%. Therefore, any QPTs below 2.8% in [GAB906] produced uncertainty components below the [PID892] uncertainties, and any QPTs above 2.8% in [GAB906] had to be bound by an additional set of uncertainties. The fact that full core SIMULATE-3 reproduces QPTs in excess of 5% without any additional uncertainty penalty proves the additional uncertainties derived in [GAB906] for QPTs above 2.8% are no longer necessary.